EurJIC European Journal of Inorganic Chemistry

MICROREVIEW

DOI: 10.1002/ejic.201101226

Synthesis and Physicochemical Characterisation of Gd-DTPA Derivatives as Contrast Agents for MRI

Sophie Laurent,[a] Céline Henoumont,[a] Luce Vander Elst,[a] and Robert N. Muller*[a,b]

Keywords: Gadolinium / Imaging agents / Relaxivity / NMRD profiles / Paramagnetic complexes

Paramagnetic magnetic resonance imaging (MRI) contrast agents are the compounds most used in clinical studies. Among these, the derivatives of Gd-DTPA (gadolinium diethylenetriaminepentaacetic acid, Magnevist®, Bayer HealthCare) have been extensively studied. The first part of this work consists of a comparison of various derivatives of Gd-DTPA [mono-, bis- or pentaamides; *C*-functionalised (C_2, C_4, C_5, N_6) or diester derivatives] according to their synthesis and to the most important parameters that regulate their efficacy. The synthesis of bis(amide)s consists of only one step and is thus easier than the synthesis of the C_4 derivatives, which needs several steps and requires a tedious purification. These last compounds are, however, more stable against transmetallation with another ion such as zinc [more than 50 % of the gadolinium complex remains after 4300 min while this percentage falls under 40 % for most of the bis-(amide) compounds] and generally have higher relaxivities. Moreover, the residence time of the water molecule in the first coordination sphere of the gadolinium complex (τ_M) is shorter for the C_4 derivatives and does not limit the relaxivity. In the second part of this work, an overview of different kinds of recently developed paramagnetic contrast agents is presented: new systems to improve the relaxivity, like fullerenol compounds, apoferritin or zeolite complexes, lipophilic complexes (in structures like micelles or liposomes), macromolecular products as well as small complexes interacting with human serum albumin (HSA).

1. Introduction

The development of magnetic resonance imaging (MRI) as a clinical diagnostic modality has prompted the need for new products to improve the contrast between healthy and diseased tissues. Among these products, any paramagnetic substances are likely to be used as MRI contrast agents because of their ability to accelerate efficiently the relaxation rate of the water protons in the regions of the body where they are accumulated. In particular, some transition metals and lanthanide ions possess single electrons and therefore accelerate efficiently the water proton relaxation rates. So far, the most used paramagnetic ion is indisputably the gadolinium ion. It possess seven unpaired electrons, which are responsible for a high magnetic moment; moreover, it has a symmetric electronic ground state (S^8) leading to a long electronic relaxation time and thus to an efficient interaction of the water protons with the gadolinium ion. Nevertheless, its medical use is proscribed because of its toxicity. This paramagnetic ion is therefore complexed to an organic ligand in order to obtain a stable and nontoxic chelate. The biological and chemical inertness of these complexes therefore constitutes one of the criteria for their clinical use.

Today, it can be estimated that 30% of clinical procedures make use of a contrast agent. Among the molecules that have received clinical approval, we find nine gadolinium complexes, in which the gadolinium ion is chelated either by a linear organic ligand, derivatised from DTPA (diethylenetriaminepentaacetic acid), or by a cyclic organic ligand, derivatised from DOTA (tetraazacyclododecanetraacetic acid) (Scheme 1).

Since the clinical approval of the first MRI contrast agent, Gd-DTPA (Magnevist®), in 1988, there has been extensive research towards new organ- and tissue-specific contrast agents. The products of the first generation, such as Gd-DTPA (Magnevist®), Gd-DTPA-BMA (Omniscan®), Gd-DOTA (Dotarem®) or Gd-HPDO3A (Prohance®) are indeed nonspecific. They are distributed in the extracellular fluid and eliminated via glomerular filtration.

The introduction of a lipophilic substituent on the skeleton of Gd-DTPA has made it possible to obtain hepatobiliary agents that target the hepatocytes. Examples are Gd-BOPTA (Multihance®) and Gd-EOB-DTPA (Eovist®).[1,2] These amphiphilic complexes allow the detection of small hepatic lesions such as metastases and confirm the good health of the hepatocytes.

Intravascular contrast agents, which consist of high-molecular-weight molecules, have also been produced. As a first strategy, the covalent coupling of the existing small

[a] Department of General, Organic and Biomedical Chemistry, NMR and Molecular Imaging Laboratory, University of Mons, Avenue Maistriau 19, Mendeleev Building, 7000 Mons, Belgium
Fax: +32-65373533
[b] Center for Microscopy and Molecular Imaging, Rue Adrienne Bolland 8, 6041 Charleroi, Belgium
E-mail: robert.muller@umons.ac.be

gadolinium complexes with a natural or a synthetic macromolecule has been considered. These macromolecules can be polymers, dendrimers, or various endogenous or exogenous macromolecular precursors, like a protein,[3] a polysaccharide[4] or a monoclonal antibody.[5] As a second strategy, the noncovalent interaction between small gadolinium complexes and an endogenous macromolecular compound, like human serum albumin (HSA), has also led to the elaboration of contrast agents with a vascular tropism.[6–8] This was successfully achieved in the case of MS-325 (AngioMARK®, Vasovist®). Finally, we can also mention the preparation of gadolinium chelates of medium size (M_w ≈ 5–6 kDa).[9,10] Thanks to their longer remanence time in the blood system, all of these compounds are suitable to perform angiography or to evaluate the tissue perfusion.

Another important class of contrast agents aim to target a specific pathology. They are often qualified as "molecular" contrast agents, because these compounds are designed to target a specific molecule that is expressed or overexpressed in a specific disease. Thus, they act according to the principle of recognition between a specific ligand and its receptor, which guarantees a high selectivity. This strategy has been, for example, extensively used to target tumours, with the hope of being able to detect them at a very early stage. This approach was successfully applied in nuclear medicine, where DTPA was substituted by different peptides[11] or other molecules like somatostatin[12] or folate,[13] which have a high affinity for tumours. However, it is more difficult to implement in the context of magnetic resonance imaging. Most of the target molecules are indeed present in the body in very small amounts (ca. 10^{-9} to 10^{-13} grammes of receptors per gramme of tissue), which makes necessary the use of a very sensitive probe to detect them. While the radioisotopes that are used in nuclear medicine are known to be very sensitive,[14] this is not the case for the present MRI contrast agents. This lack of sensitivity is thus, at pres-

Sophie Laurent was born in 1967. Her studies were performed at the University of Mons-Hainaut (Belgium), where she received her Ph. D. in chemistry in 1993. She then joined Prof. R. N. Muller's team and was involved in the development (synthesis and physicochemical characterisation) of paramagnetic Gd complexes and superparamagnetic iron oxide nanoparticles as contrast agents for MRI. She is currently working on the vectorisation of contrast agents for molecular imaging. She is a lecturer and co-author of around 120 publications and more than 200 communications in international meetings.

Céline Henoumont was born in 1982 and studied at the University of Mons (Belgium), where she obtained her Ph. D. in chemistry in 2008. She is now assistant in Prof. R. N. Muller's team and continues her research on the characterisation of MRI contrast agents by NMR spectroscopy. She is a co-author of 7 publications and around 30 communications in national and international meetings.

Luce Vander Elst was born in 1955. She studied at the University of Mons-Hainaut, where she obtained her Ph. D. degree in 1984. She did postdoctoral research on the multinuclear NMR spectroscopic analysis of the metabolism of perfused mammalian hearts at the Medical School of Harvard University in 1986. She works as a professor in the NMR and Molecular Imaging Laboratory of the University of Mons. Her research focuses mainly on high-resolution NMR spectroscopic and physicochemical characterisation of magnetic resonance imaging (MRI) and optical imaging (OI) contrast agents.

Robert N. Muller was born in 1948 and studied at the University of Mons-Hainaut (UMH), Belgium, where he graduated with a M. Sc. Degree in chemistry in 1969. He obtained his Ph. D. in 1974 from the same university, where he was successively appointed assistant, lecturer and full professor. Currently head of the Department of General, Organic and Biomedical Chemistry, he is, since October 2005, dean of the Faculty of Medicine and Pharmacy of the University of Mons. He did post-doctoral studies on MRI in Paul C. Lauterbur's research group at the State University of New York at Stony Brook in 1981–1982, collaborated with Dr. Seymour Koenig in the domain of fast field cycling relaxometry and was on a sabbatical leave at the Centre for Magnetic Resonance (CERM), Florence, Italy, with Professors Ivano Bertini and Claudio Luchinat in 2002–2003. He is co-founder of the European Workshop on Nuclear Magnetic Resonance in Medicine, vice-chairman of the European Magnetic Resonance Forum Foundation (1991–present), president of the European Society for Magnetic Resonance in Medicine and Biology (1987–1988), president of the Groupe de Recherche sur les Applications du Magnétisme en Médecine (GRAMM; 1998–2000), vice-chairman of the COST D18 Action (2003), founding member of the European Society for Molecular Imaging (ESMI), editor in chief of the new journal Contrast Media and Molecular Imaging (Wiley) and a member of the editorial boards of Magnetic Resonance Materials MAGMA (Springer) and Investigative Radiology (Lipincott). He has produced around 200 publications and contributed to six books mainly in NMR relaxometry, spectroscopy and imaging in the context of the development and applications of contrast agents for molecular imaging.

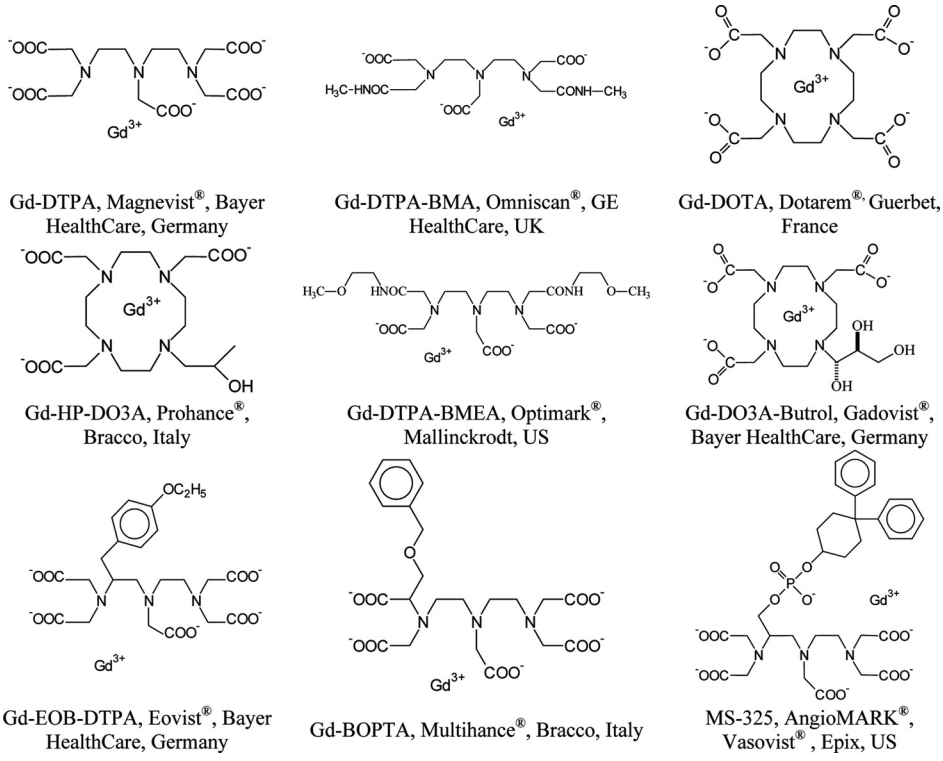

Scheme 1. Structures of the nine clinical Gd complexes.

ent, a brake on the development of molecular contrast agents for MRI.

Increasing the sensitivity of MRI contrast agents is thus an important challenge, and this explains the numerous studies performed in recent years on this subject. Among these studies, those on *N*- or *C*-functionalised derivatives of Gd-DTPA have received a lot of attention.[15–19] This work summarises the synthetic schemes for each of these derivatives as well as their physicochemical properties.

The thermodynamic stability constants of Gd complexes (Gd-DTPA, Gd-EOB-DTPA or Gd-BOPTA) are very large ($\log K > 20$). The conversion of one carboxylate group into an amide or an ester results in a decrease in the stability of the new Gd compound by about three orders of magnitude.[20] Thus, the removal of one carboxylate group (anionic donor atom) and its replacement by an amide or ester function (non-ionic group) results in a less stable complex. For example, the stability constants ($\log K$) of Gd-DTPA-BMA and Gd-DTPA-BPE {bis(propyl ester)} are 16.85 and 16.23, respectively. The suitability of gadolinium complexes as MRI contrast agents depends also on their inertness towards transmetallation with endogenous ions, such as Cu^{2+}, Ca^{2+} and Zn^{2+}.[21–23] Among these, only the zinc(II) ion can displace a significant amount of gadolinium, since its concentration in blood is relatively high (55 to 125 μM) and its association constant with EDTA, DTPA or DOTA is only about four orders of magnitude lower than that of the gadolinium(III) ion.[24] The stability of Gd complexes in the presence of Zn^{2+} is thus an important issue, because the transmetallation process will induce a release of gadolinium ions into the body and a possible depletion of the endogenous ion subsequent to its elimination as a hydrophilic complex through the kidneys.

2. Relaxation Mechanisms of Water Protons in the Presence of a Gadolinium Chelate

The small gadolinium chelates decrease both the longitudinal and transverse relaxation times (T_1 and T_2) of the nearby water protons. They are nevertheless often considered as T_1 contrast agents, because their effect is much more marked on the longitudinal relaxation time (T_1) of tissues at the magnetic fields usually used in MRI (0.5–3T). That is why the following discussion is focused on the longitudinal relaxation time of the water protons.

The efficacy of a gadolinium chelate, usually defined as the longitudinal relaxivity (r_1), which represents the increase in the longitudinal water proton relaxation rate induced by one millimole per litre of gadolinium chelate, is linked to its molecular movements but also to the intrinsic relaxation properties of the unpaired electrons of the gadolinium ion. Two contributions can be distinguished for most of the small gadolinium complexes: the inner sphere mechanism (IS), which concerns the water molecule(s) bound to the first coordination sphere of the gadolinium ion, and the outer sphere mechanism (OS), which regards the water molecules diffusing near the gadolinium ion.[25] For some contrast agents, a few water molecules can remain close to the gadolinium ion for a relatively long time as a result of

the formation of hydrogen bonds with the organic ligand or with the water molecule(s) in the first coordination sphere of the gadolinium ion. This additional contribution to the paramagnetic relaxation rate of the water protons, called the second-sphere mechanism, can be described by the same equations as those for the inner sphere contribution.[26] This term is often neglected, but there are some examples where it has to be taken into account in order to adjust the experimental data correctly.

The principle of inner sphere relaxation (Scheme 2) is a chemical exchange between the water molecules in the first coordination sphere of the gadolinium ion and the water molecules of the bulk. This mechanism, which can be represented by an exchange of the water molecules between two sites, allows the propagation of the paramagnetic effect to the bulk water. It was described by the Solomon–Bloembergen–Morgan theory (SBM).[27] The inner sphere contribution can be expressed by Equation (1).

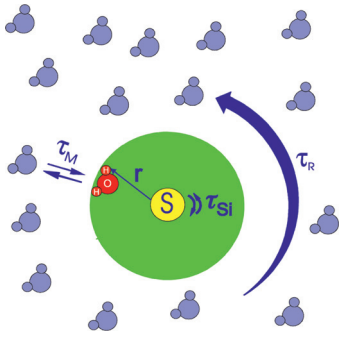

Scheme 2. Schematic representation of the inner sphere mechanism.

$$R_1^{IS} = fq\frac{1}{T_{1M}+\tau_M} \quad (1)$$

where f is the molar fraction of the paramagnetic complex, q is the number of water molecules in the first coordination sphere, τ_M is the residence time of water in the first coordination sphere and T_{1M} is the longitudinal relaxation time of the coordinated water molecule(s).

The relaxation of the coordinated water molecule(s), T_{1M}, is governed by a dipolar and a scalar mechanism. The latter is a mechanism of contact, where the electrons of the paramagnetic ion are delocalised on the protons of the coordinated water molecule(s), and this is never observed in the case of the gadolinium ion. As the scalar term can be neglected, the relaxation of the coordinated water molecules can be expressed by Equation (2).

$$\frac{1}{T_{1M}} = \frac{1}{T_{1M}^{DD}} = \frac{2}{15}\left(\frac{\mu_0}{4\pi}\right)^2 \gamma_H^2\gamma_S^2\hbar^2 S(S+1)\frac{1}{r^6}\left[\frac{7\tau_{c2}}{1+(\omega_S\tau_{c2})^2}+\frac{3\tau_{c1}}{1+(\omega_H\tau_{c1})^2}\right] \quad (2)$$

where γ_S and γ_H are the gyromagnetic ratios of the electron (S) and of the proton (H), respectively, ω_S and ω_H are the Larmor frequencies of the electron and of the proton, respectively, r is the distance between the coordinated water protons and the unpaired electrons, and τ_{ci} are the correlation times modulating the interaction. These are defined by Equation (3).

$$\frac{1}{\tau_{ci}} = \frac{1}{\tau_R}+\frac{1}{\tau_M}+\frac{1}{\tau_{si}} \quad (3)$$

where $i = 1, 2$. Here τ_R is the rotational correlation time of the hydrated complex and τ_{Si} are the longitudinal (τ_{S1}) and transverse (τ_{S2}) relaxation times of the electrons of the gadolinium ions. These latter parameters are field-dependent and can be expressed by Equations (4) and (5) or Equations (6) and (7), according to the model of Bloembergen–Morgan: τ_{S0} is the electronic relaxation time at zero field and depends on the tensor of the zero-field splitting (ZFS) and τ_V is the correlation time for the modulation of the ZFS.

$$\frac{1}{\tau_{S1}} = \frac{1}{5\tau_{S0}}\left[\frac{1}{1+\omega_S^2\tau_V^2}+\frac{4}{1+4\omega_S^2\tau_V^2}\right] \quad (4)$$

$$\frac{1}{\tau_{S2}} = \frac{1}{10\tau_{S0}}\left[3+\frac{5}{1+\omega_S^2\tau_V^2}+\frac{2}{1+4\omega_S^2\tau_V^2}\right] \quad (5)$$

or

$$\frac{1}{\tau_{S1}} = B\tau_v\left[\frac{1}{1+\omega_S^2\tau_V^2}+\frac{4}{1+4\omega_S^2\tau_V^2}\right] \quad (6)$$

$$\frac{1}{\tau_{S2}} = \frac{B\tau_v}{2}\left[3+\frac{5}{1+\omega_S^2\tau_V^2}+\frac{2}{1+4\omega_S^2\tau_V^2}\right] \quad (7)$$

where $B = \dfrac{\Delta^2\{4S(S+1)-3\}}{25}$ and Δ^2 depends on the trace of the square of the ZFS tensor.

Outer sphere relaxation comes from the water molecules that diffuse freely in the vicinity of the gadolinium ion and can consequently interact with it (Scheme 3). This mechanism, which does not require any binding between the two species, is governed by the relative motion of the two molecules and their distance of closest approach. The time modulation characterising this interaction, named the diffusion correlation time τ_D, is given by Equation (8).

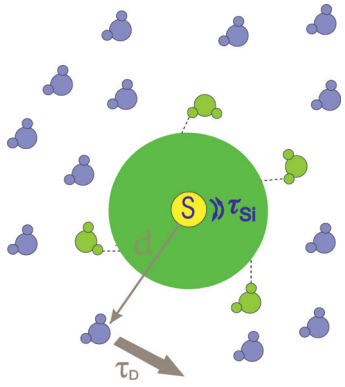

Scheme 3. Schematic representation of the outer sphere relaxation.

$$\tau_D = d^2/(D_H + D_S) = d^2/D \quad (8)$$

where d is the distance of closest approach between the protons of the diffusing water molecules and the gadolinium ion, and D_H and D_S are the molecular diffusion coefficients of water and of the paramagnetic centre, respectively.

The outer sphere relaxation, which was described by Freed,[28] is given by Equations (9) and (10).

$$R_1^{os} = \frac{32\pi}{405}\gamma_H^2\gamma_S^2\hbar^2 S(S+1)NA\frac{[C]}{dD}[7j(\omega_S\tau_D) + 3j(\omega_H\tau_D)] \quad (9)$$

$$j(\omega\tau_D) = \mathrm{Re}\left[\frac{1+\frac{1}{4}(i\omega\tau_D + \tau_D/\tau_{SI})^{1/2}}{1+(i\omega\tau_D + \tau_D/\tau_{SI})^{1/2} + \frac{4}{9}(i\omega\tau_D + \tau_D/\tau_{SI}) + \frac{1}{9}(i\omega\tau_D + \tau_D/\tau_{SI})^{3/2}}\right] \quad (10)$$

In these equations, [C] is the molar concentration of the paramagnetic ion and NA is Avogadro's number.

The above equations are very complicated and depend on a high number of parameters. Some of them can be estimated independently, which is a great help in the characterisation of the relaxation properties of the small gadolinium chelates.

2.1. The Rotational Correlation Time τ_R

The rotational correlation time (τ_R) characterises the reorientation of the hydrated complex, or more precisely the reorientation of the Gd^{3+}–proton vector of the water molecule(s). This parameter has a strong influence on the relaxivity of the gadolinium complexes at the magnetic fields used in MRI (0.5–3 T). At these fields, it can indeed be shown that the increase in τ_R caused by an increase in the molecular weight of the gadolinium chelates will greatly raise their relaxivity. The efficacy of most of the small gadolinium complexes is thus notably limited by τ_R at the fields used in MRI.

The rotational correlation time can be measured by several methods[15] such as: (1) analysis of the ^{17}O longitudinal relaxation rate of water in a solution of the gadolinium complex, (2) measurement of the longitudinal relaxation rate of ^{13}C in a solution of a diamagnetic analogue of the gadolinium chelate, (3) fluorescence polarisation spectroscopy, which requires the introduction of a suitable fluorophore on the gadolinium complex, (4) EPR spectra of complexes in which the gadolinium ion is substituted by the vanadyl ion VO^{2+}[29] or (5) measurement of the deuterium longitudinal relaxation rate in a solution of the diamagnetic analogue of the gadolinium chelate previously labelled with deuterium. All of these techniques present some advantages and some inconveniences, but for the study of the small derivatives of Gd-DTPA, the use of the deuteriated diamagnetic analogue of the gadolinium chelate (i.e. the lanthanum chelate) seemed to be the most appropriate method to assess the value of τ_R. This was performed by labelling the methylene group in the α-position of the carbonyl or carboxyl functions of DTPA. For these small diamagnetic complexes, the longitudinal relaxation rate of the deuterium nucleus is given by Equation (11), where the quantity in the brackets is the quadrupolar coupling constant. This constant depends on the degree of hybridisation of the carbon atom bound to the deuterium and is equal to 170 kHz for an sp^3 carbon atom. The measurement of the longitudinal relaxation rate of the deuterium thus provides directly the information about the rotational correlation time of the complex.

$$R_1 = \frac{1}{T_1} = \frac{3}{8}\left(\frac{e^2qQ}{\hbar}\right)^2\tau_R \quad (11)$$

2.2. The Electronic Relaxation Times τ_{S1} and τ_{S2}

The longitudinal and transverse electronic relaxation times, τ_{S1} and τ_{S2}, respectively, refer to the relaxation times of the unpaired electrons associated with the gadolinium ion. These relaxation times are usually attributed to a transient ZFS, produced by solvent collisions or molecular vibrations, which induce distortions in the symmetrical electronic ground state of the gadolinium ion.

Electronic relaxation rates are field-dependent, as shown by Equations (4) and (5). For the gadolinium complexes, τ_{S1} increases from 8×10^{-11} s at 0.01 MHz to 2×10^{-6} s at 1000 MHz and τ_{S2} increases from 8×10^{-11} s at 0.01 MHz to 3×10^{-10} s at 1000 MHz. In comparison with the values of τ_R (some tens of picoseconds for the small gadolinium complexes) and τ_M (from some tens of nanoseconds to a thousand nanoseconds, depending on the structure of the gadolinium chelate), the influence of τ_{S2} will be marked particularly at low field.

2.3. The Number of Coordinated Water Molecules *q*

Inner sphere relaxivity is directly proportional to the number of coordinated water molecules [see Equation (1)].

An increase in this number will thus greatly increase the inner sphere contribution. It can indeed be shown that complexes with a structure derivatised from that of Gd-DTPA, with two coordinated water molecules, have approximately 30% higher relaxivity in comparison with chelates characterised by one coordinated water molecule. Unfortunately, most of the gadolinium chelates that have more than one coordinated water molecule are often characterised by a decrease in the kinetic inertia of the chelate.

The evaluation of this number (q) can be performed by several methods, out of which two kinds of measurements can be distinguished: measurements (1) in the solid phase and (2) in solution. The measurements in the solid phase are obtained by classical diffraction techniques (X-ray diffraction and neutron diffraction). In solution, a first method is laser-induced luminescence of the Eu^{III} or Tb^{III} complexes.[30] The ratio of the fluorescence lifetimes of these complexes measured in H_2O and D_2O is indeed related to q. A second method takes advantage of the LIS (lanthanide-induced shift). The dysprosium-induced shift of the ^{17}O water resonance in the analogous Dy^{III} chelates, which is indeed proportional to q, was first used,[31a] but it has been reported that the LIS induced by the Gd chelates can also be used.[31b]

2.4. The Proton–Metal Distance r

This parameter occurs at its sixth power in the expression for the relaxation rate of the coordinated water molecule [see Equation (2)]. It thus has a strong influence on the inner sphere relaxivity. Indeed, a quick calculation shows that a decrease of 0.1 Å in the proton–metal distance induces an increase of 20% in the inner sphere relaxation rate.

This parameter is very difficult to measure, but according to the results of several crystallographic studies, it is equal to 0.31 ± 0.01 nm. It can, for example, be shown that the C_4 derivatives of Gd-DTPA are characterised by a distance r of 0.30 nm, in contrast to the other derivatives of Gd-DTPA (r = 0.31 nm). This reduction could be in part responsible for the higher relaxivity of Gd-EOB-DTPA (5.5 $mM^{-1}s^{-1}$ at 310 K and 20 MHz) compared to that of Gd-DTPA (3.9 $mM^{-1}s^{-1}$ at 310 K and 20 MHz).[6,7]

2.5. The Coordinated Water Exchange Rate τ_M

The mechanism of inner sphere relaxation is based on an exchange between the water molecule(s) coordinated to the lanthanide ion and the water molecules of the bulk. Consequently, the exchange rate ($k_{ex} = 1/\tau_M$) is an essential parameter for the transmission of the "relaxing" effect on the solvent.

The principle of the measurement is based on the works of Swift and Connick for diluted paramagnetic solutions[32] and consists of the analysis of the variation of the ^{17}O transverse relaxation rate of water with temperature. The ^{17}O water paramagnetic transverse relaxation rate for solutions of Gd complexes is given by Equation (12) where T_{2M}, the transverse relaxation rate of the water oxygen atom bound to the gadolinium ion, results from a scalar interaction between the electrons and the oxygen nucleus [Equation (13)]. The ^{17}O chemical shift of the water molecule, $\Delta\omega_M$, is given by Equation (14). The outer sphere contribution can be neglected.[33]

$$\frac{1}{T_2^{is}} = fq\frac{1}{\tau_M}\frac{\frac{1}{T_{2M}^2}+\frac{1}{\tau_M T_{2M}}+\Delta\omega_M^2}{\left(\frac{1}{\tau_M}+\frac{1}{T_{2M}}\right)^2+\Delta\omega_M^2} \quad (12)$$

$$\frac{1}{T_{2M}} = \frac{1}{3}S(S+1)\left(\frac{A}{\hbar}\right)^2\left[\tau_{e1}+\frac{\tau_{e2}}{1+\omega_S^2\tau_{e2}^2}\right] \quad (13)$$

$$\Delta\omega_M = \frac{g_L\mu_B S(S+1)B_o}{3k_B T}\frac{A}{\hbar} \quad (14)$$

$A/\hbar$ is the hyperfine or scalar coupling constant between oxygen and Gd^{3+} and τ_{ei} values are given by $[\tau_M^{-1} + \tau_{Si}^{-1}]^{-1}$. The Landé factor, g_L, is equal to 2.0 for Gd^{3+}; μ_B is the Bohr magneton, B_0 is the external magnetic field and k_B is the Boltzmann constant.

The temperature dependences of τ_M and τ_V can be described by Equations (15) and (16), respectively.

$$\frac{1}{\tau_M} = \frac{k_B T}{h}\exp\left(\frac{\Delta S^{\neq}}{R}-\frac{\Delta H^{\neq}}{RT}\right) \quad (15)$$

$$\tau_V = \tau_V^{298}\exp\left(\frac{E_V}{R}\left(\frac{1}{T}-\frac{1}{298.15}\right)\right) \quad (16)$$

$\Delta S^{\neq}$ and $\Delta H^{\neq}$ are the entropy and enthalpy of activation for the water exchange process, τ_V^{298} is the correlation time at 298.15 K, and E_V is the activation energy for this process.

According to those equations, the measurement of the reduced transverse relaxation rate of ^{17}O [$1/T_2^r = (1/T_2^{IS})/(fq)$] at different temperatures allows the estimation of τ_M as well as other parameters {$\Delta S^{\neq}$, $\Delta H^{\neq}$, τ_V^{298}, E_V, $A/\hbar$ and B [see Equations (6) and (7)]}. An example is shown in Figure 1, where the curves for three different gadolinium complexes are displayed. It clearly illustrates that τ_M can be very different according to the structure of the chelate.[34] That is why this parameter has been extensively measured in many complexes[33,35–39] including the derivatives of Gd-DTPA. The results obtained are presented below.

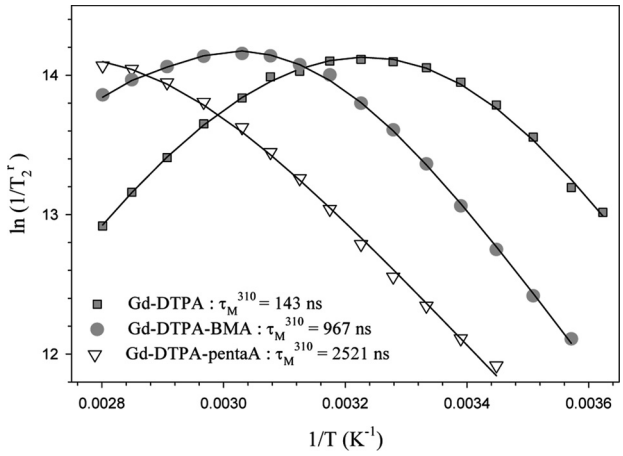

Figure 1. ^{17}O reduced transverse relaxation rate ($1/T_2^r$) as a function of the reciprocal of the temperature for aqueous solutions of various Gd complexes (B_0 = 7.5 T).

3. Synthesis and Relaxometric Characterisation of Different *N*-, *O*- and *C*-Functionalised Derivatives of Gd-DTPA

The study of the properties of contrast agents and the knowledge of all the parameters influencing their relaxivity make it possible not only to predict but also to improve their efficacy. This review therefore aims to summarise the relaxometric properties of different derivatives of Gd-DTPA.

3.1. General Synthesis Methods, Materials and Instrumentation

The synthesis of the different *N*-, *O*- and *C*-functionalised derivatives of DTPA is described below. The different gadolinium complexes are prepared by mixing equimolar amounts of ligand and gadolinium chloride ($GdCl_3 \cdot 6H_2O$). The pH value is monitored between 5.5 and 6.5 with sodium hydroxide. The aqueous solution of the complex thus contains also a variable amount of sodium chloride salt, and consequently desalting is sometimes necessary.

A rapid method to observe the formation of the complex is electrospray mass spectrometry (ES-MS). The proton molecular ions or their sodium adducts are indeed characteristic thanks to the high number of gadolinium isotopes (see an example in Figure 2). The xylenol orange and the arsenazo tests are also usually used to confirm the absence of free gadolinium(III) ions.[40] At the end, the final concentration of the gadolinium complex is determined by relaxometry or ICP.

The relaxometric properties of the gadolinium complexes are usually determined by the NMRD (proton nuclear magnetic relaxation dispersion) curves, which display the relaxivity of the gadolinium chelate with respect to the magnetic field. The theoretical adjustment of these curves with the above equations makes it possible to extract the different parameters influencing the relaxivity of the gadolinium chelates. Some of them are, however, similar for all the

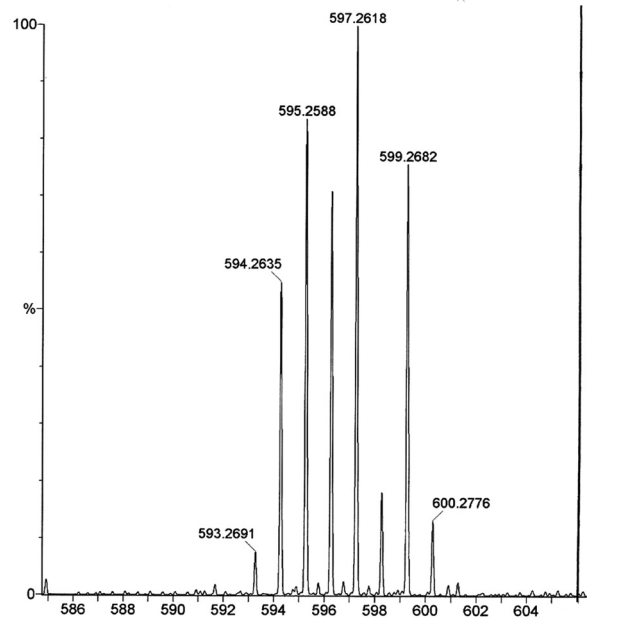

Figure 2. Mass spectrum of Gd-DTPA-BMA. The different peaks correspond to the sodium adducts of the complex ($[M + Na]^+$), each peak representing an adduct with an isotope of the gadolinium ion.

derivatives of Gd-DTPA and are thus fixed during the fitting of the data: the number of coordinated water molecules (q) is equal to one; the distance between the protons of the coordinated water molecules and the gadolinium ion (r) is equal to 0.31 nm for most of the small gadolinium chelates and it is equal to 0.30 nm for the *C*-functionalised derivatives of Gd-DTPA; the distance of closest approach for the water molecules (d) is equal to 0.36 nm, and the relative diffusion coefficient (D) is close to that of pure water and is thus equal to 3×10^{-9} $m^2 s^{-1}$ at 310 K. The other parameters, that is, the residence time of the coordinated water molecule (τ_M), the rotational correlation time of the chelate (τ_R), the electronic relaxation time at very low fields (τ_{S0}) and the correlation time describing the modulation of the ZFS (τ_V) depend on the structure of the gadolinium complex. Considering such a high number of parameters, the determination of some of them by independent techniques is very useful. In our case, the estimation of τ_M and τ_R was performed independently, when possible, as described above, that is, by ^{17}O and ^2H NMR spectroscopy, respectively. The other parameters were extracted from the NMRD curves (Tables 1–10).

All of the NMRD curves were obtained at 310 K with a Stelar (PV, Mede, Italy) or an IBM relaxometer (Field Cycling Systems, Honesdale, PA, USA). Additional relaxation rates at 0.47, 1.4 and 7.05 T were obtained at 310 K with a Minispec PC-120, Mq-60 and Bruker AMX-300 spectrometer, respectively (Bruker, Karlsruhe, Germany). The fitting of the ^1H NMRD curves was performed with a data-processing software, which uses different theoretical models describing nuclear relaxation phenomena (Minuit, CERN Library).[41,42]

The transmetallation phenomenon was analysed through the evolution of the paramagnetic longitudinal relaxation rate of water protons at 37 °C in phosphate buffer solutions (pH = 7) containing the Gd complexes (2.5 mM) and zinc chloride (2.5 mM). The measurements were performed at 0.47 T over a period of at least three days.[43]

3.2. Gd-DTPA

The NMRD curve for the parent compound, Gd-DTPA, is depicted in Figure 3, and its relaxometric parameters are presented in Table 1.

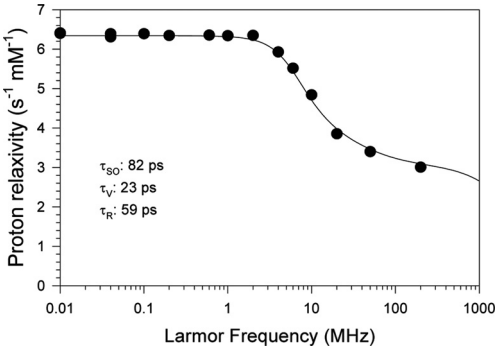

Figure 3. NMRD profile of the parent compound Gd-DTPA (T = 310 K).[19]

Table 1. Relaxometric parameters of Gd-DTPA (**1**) at 310 K.

r_1^{310} at 20 MHz (s^{-1} mM^{-1})	τ_M^{310}[a] (ns)	τ_R^{310}[a] (ps)	τ_{S0}^{310} (ps)	τ_V^{310} (ps)	Transmetallation (%)[b]
3.9	143	59	82	23	51

[a] τ_M and τ_R were independently determined by ^{17}O NMR and ^2H NMR spectroscopy, respectively, as explained previously. [b] Percentage of transmetallated gadolinium complex after 4500 min.

3.3. *N*-Functionalised Derivatives of Gd-DTPA

3.3.1. Gd-DTPA-Bis(amide)s

Gd-DTPA-bis(amide) complexes are the most studied class of contrast agents, probably because of their easy synthesis. The ligand can indeed be prepared in two steps: DTPA-bis(anhydride), obtained by heating DTPA with acetic anhydride in pyridine,[44] reacts with the corresponding amine (Scheme 4). To increase the yield of the reaction, DTPA-bis(anhydride) is prepared just before the reaction with the amine, which is performed in DMF[45,46] or water.[47,48]

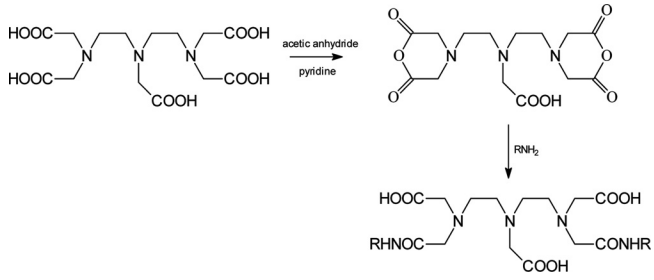

Scheme 4. Synthesis of DTPA-bis(amide)s.

This protocol was applied to obtain a series of DTPA-bis(amide)s with aliphatic linear chains from C_1 to C_7, as well as their isomers[49] with amino acids[50] and with glycosylated derivatives.[51] Their structures are presented in Table 2.

As a particular case, the DTPA-BhydroxyA ligand was obtained by reaction of DTPA-bis(hexylthioester) with hydroxamic acid. The bis(thioester) ligands can be synthesised from DTPA-bis(anhydride) and the corresponding thioalcohol in anhydrous DMF in the presence of 4-dimethylaminopyridine (Scheme 5).[28]

The synthesis of Gd-DTPA-bis(amide)s with amino acids presents an additional difficulty because of the reduced solubility of amino acids in organic solvents. The addition of an aqueous acid solution to DTPA-bis(anhydride) is thus mandatory, but this leads to a mixture containing DTPA, DTPA-bis(amide) and DTPA-monoamide. The DTPA-bis(amide) can be isolated by ion exchange chromatography.[50]

The last compound in Table 2, [Gd-DTPA-B(Slex)A], aims to target inflammation, during which endothelial cells solicit leucocytes via cell adhesion molecules such as selectins. Sialyl Lewis X is a ligand of these molecules and allows the neutrophiles to recognise endothelial cells close to the inflammation area. A mimetic of that molecule, the (α-D-

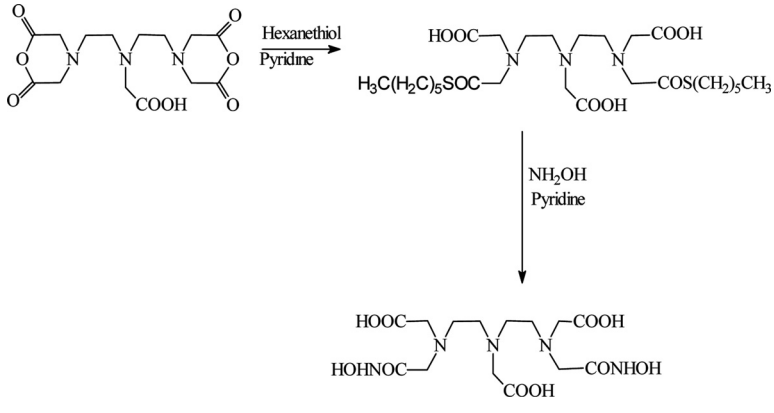

Scheme 5. Synthesis of the ligand DTPA-BhydroxyA.

Table 2. Structural and relaxometric parameters of Gd-DTPA-bis(amide)s.

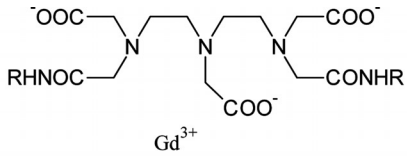

Compounds	r_1^{310} at 20 MHz (s^{-1} mM^{-1})	τ_M^{310} (ns)[a]	τ_R^{310} (ps)	τ_{S0}^{310} (ps)	τ_V^{310} (ps)
Gd-DTPA **1**	3.9	143	59[b]	82	23
Gd-DTPA-BA **2** (R = H)	3.6	1171	61[b]	99	16
Gd-DTPA-BMA **3** (R = CH_3)	3.8	967	69[b]	84	16
Gd-DTPA-BEA **4** (R = C_2H_5)	3.7	927	70[b]	84	11
Gd-DTPA-BPA **5** (R = *n*-C_3H_7)	4.0	845	74	83	14
Gd-DTPA-BiPA **6** (R = *iso*-C_3H_7)	4.1	654	80	95	25
Gd-DTPA-BHPA **7** R = $CH_2CHOHCH_3$	4.5	1128	102[b]	106	30
Gd-DTPA-BnBA **8** (R = *n*-C_4H_9)	4.4	713	82[b]	83	19
Gd-DTPA-BiBA **9** (R = *iso*-C_4H_9)	4.6	660	80[b]	80	19
Gd-DTPA-BtBA **10** (R = *tert*-C_4H_9)	4.2	659	91	95	16
Gd-DTPA-BAA **11** (R = C_5H_{11})	4.3	575	107	96	29
Gd-DTPA-BHA **12** (R = C_6H_{13})	4.5	681	94[b]	99	31
Gd-DTPA-BcHA **13** (R = cyclohexyl)	4.3	584	87[b]	76	18
Gd-DTPA-BheptA **14** (R = C_7H_{15})	4.5	673	109	89	24
Gd-DTPA-BBzA **15** (R = benzyl)	4.3	305	70[b]	96	22
Gd-DTPA-BbutPheA **16** R = $(CH_2)_4$-phenyl	4.7	686	99[b]	80	23
Gd-DTPA-BAlaA **17** R = 	4.5	836	96	83	20
Gd-DTPA-BLeuA **18** R = 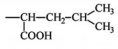	4.9	477	96	96	27
Gd-DTPA-BHisA **19** R = 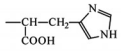	4.5	756	88	87	19
Gd-DTPA-BhydroxyA **20** (R = OH)	4.0[c]	824	72	114	32
Gd-DTPA-Bglucosamide **21** R = 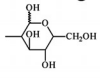	4.9	1757	91[b]	71	15
Gd-DTPA-glucamide **22** R = 	4.8	1213	103	88	27
Gd-DTPA-BC2-gluconA **23** R = 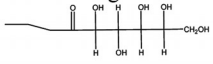	5.2	1329	135	91	31
Gd-DTPA-B(Slex)A **24** R = 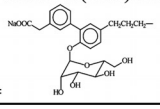	3.9	259	93	97	24

[a] τ_M was measured independently by ^{17}O NMR spectroscopy. [b] For these compounds, τ_R was measured independently by ^2H NMR spectroscopy; for the others, it was determined from the fitting of the NMRD curves. [c] This value was measured in a water solution of the complex at pH 6. The relaxivity of this gadolinium chelate is, however, pH-dependent: the values at pH 9 and 11 are 4.3 and 4.4 s^{-1} mM^{-1}, respectively.

mannopyranosyloxy)biphenyl group,[52,53] was thus grafted on Gd-DTPA through the formation of a Gd-DTPA-bis(amide). The relaxometric parameters of this compound are depicted in Table 2.

Several tertiary Gd-DTPA-bis(amide)s were also obtained by following the same protocol as that described above. Their structures and relaxometric parameters are presented in Table 3.

3.3.2. Gd-DTPA-Monoamides

Only a few Gd-DTPA-monoamides have been described in the literature,[54] and this situation can be explained by the difficulties posed by the synthesis of these compounds. Indeed, the reaction of DTPA-bis(anhydride) with an equivalent amount of amine leads to a reaction mixture in which large amounts of DTPA and DTPA-bis(amide) are present

Table 3. Structural and relaxometric parameters of secondary Gd-DTPA-bis(amide)s.

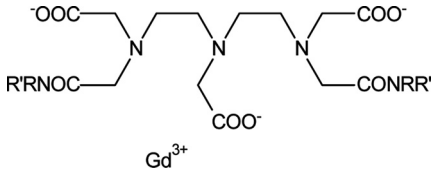

Compounds	r_1^{310} at 20 MHz (s^{-1} mM^{-1})	τ_M^{310}[a] (ns)	τ_R^{310} (ps)	τ_{S0}^{310} (ps)	τ_V^{310} (ps)
Gd-DTPA-BBMA **25** (R = R′ = CH_3)	3.8	624	70[b]	86	14
Gd-DTPA-BBEA **26** (R = R′ = C_2H_5)	4.2	654	86	92	19
Gd-DTPA-BBPA **27** (R = R′ = *n*-C_3H_7)	4.5	672	96	87	23

[a] τ_M was measured independently by ^{17}O NMR spectroscopy. [b] For this compound, τ_R was measured independently by ^2H NMR spectroscopy; for the others, it was determined from the fitting of the NMRD curves.

with the desired DTPA-monoamide. However, the purification of the DTPA-monoamides is very difficult. Some alternative methods for the synthesis of DTPA-monoamides have been proposed,[55] among which we have chosen the method of Krejcarek and Tucker[56] to activate one of the carboxyl groups with isobutyl chloroformate in acetonitrile before reaction with methylamine (Scheme 6). The DTPA-monoamides can also be obtained from DTPA-triesters or DTPA-tetraesters by reaction with the corresponding amine.[57] The structure and the relaxometric parameters of the synthesised compound are presented in Table 4.

3.3.3. Gd-DTPA-Pentaamides

The synthesis of DTPA-pentaamide derivatives can be performed from the activated pentaester, which is obtained in situ by the action of dimethylaminopyridine (DMAP), dicyclohexylcarbodiimide (DCC) and *N*-hydroxysuccinimide (NHS) on DTPA-bis(anhydride). The DTPA-pentaester can then react with the corresponding amine, which is added in excess (Scheme 7). Two derivatives have been obtained, the pentaamide and the pentamethylamide compounds. Their structures and relaxometric properties are presented in Table 5.

Table 4. Structural and relaxometric parameters of the Gd-DTPA-monoamide synthesised in our group.

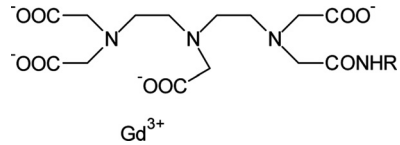

Compound	r_1^{310} at 20 MHz (s^{-1} mM^{-1})	τ_M^{310}[a] (ns)	τ_R^{310}[a] (ps)	τ_{S0}^{310} (ps)	τ_V^{310} (ps)
Gd-DTPA-MMA **28** (R = CH_3)	3.8	178	62	76	20

[a] For this compound, τ_M was measured independently by ^{17}O NMR spectroscopy, but τ_R was determined from the fitting of the NMRD curves.

As an example, the NMRD curves of some of these *N*-functionalised derivatives of Gd-DTPA are presented in Figure 4.

Comparison of Tables 2, 3 and 4 shows that the different *N*-functionalised derivatives of Gd-DTPA are characterised by a similar or higher relaxivity than that of Gd-DTPA. This increase of the observed relaxivity can be explained in most cases by an increase in the rotational correlation time τ_R due to an increase in the molecular mass of the complex. The residence time of the coordinated water molecule, τ_M, has, however, a non-negligible effect on the relaxivities of these gadolinium complexes. The obtained data show indeed a global increase in τ_M for the *N*-functionalised derivatives of Gd-DTPA relative to the value obtained for Gd-DTPA. As previously published,[18,34,49,58,59] this can be explained by the mechanism of water exchange, which is dissociative in the case of gadolinium chelates. This mechanism is indeed favoured by a steric crowding in the inner sphere of gadolinium. The replacement of one or several carboxylate functions by an amide function is thus unfavourable, because an amide group is less strongly coordinated to the gadolinium ion than a carboxylate group.

A large increase in the residence time (τ_M) of the coordinated water molecule has an influence on the relaxivities of the gadolinium complexes, especially at low magnetic field. This explains the observed NMRD profiles for the two Gd-DTPA-pentaamides, which show a lower relaxivity than the other *N*-functionalised derivatives, especially at low magnetic field.

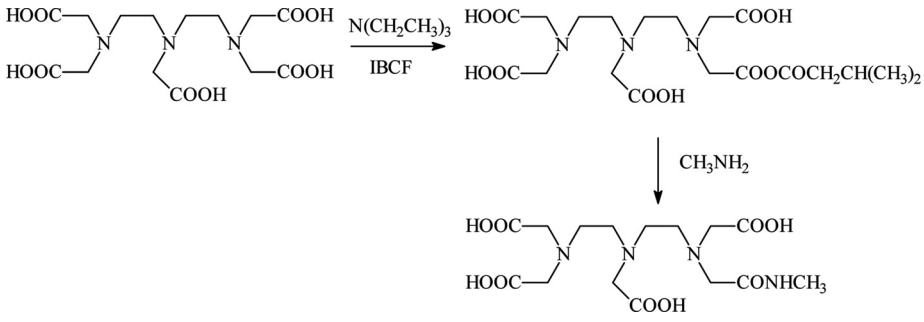

Scheme 6. Synthesis of DTPA-monoamides by the method of Krejcarek and Tucker.

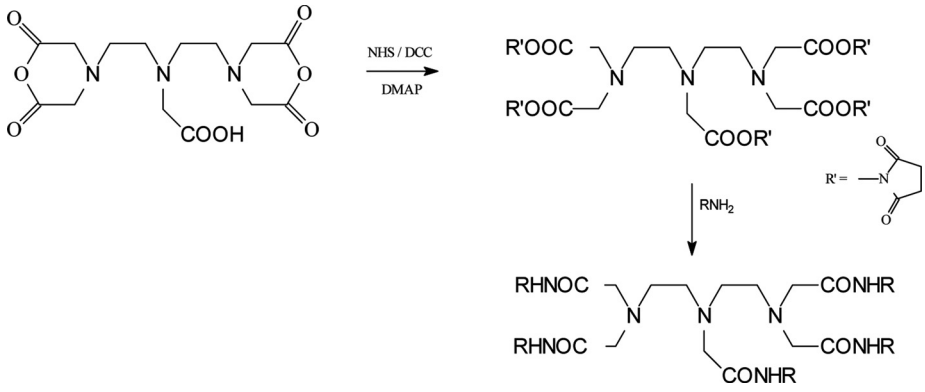

Scheme 7. Synthesis of DTPA-pentaamides.

Table 5. Structural and relaxometric parameters of two Gd-DTPA-pentaamides.

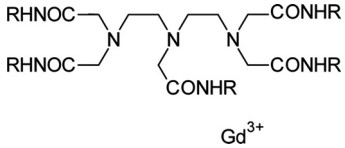

Compounds	r_1^{310} at 20 MHz (s^{-1} mM^{-1})	τ_M^{310}[a] (ns)	τ_R^{310}[a] (ps)	τ_{S0}^{310} (ps)	τ_V^{310} (ps)
Gd-DTPA-pentaA **29** (R = H)	3.0	2521	60	56	6
Gd-DTPA-pentaMA **30** (R = CH_3)	3.0	2882	65	49	6

[a] For these compounds, τ_M was measured independently by ^{17}O NMR spectroscopy but τ_R was determined from the fitting of the NMRD curves.

The transmetallation studies performed on some of those *N*-functionalised derivatives of Gd-DTPA (see Figure 5) have shown a global tendency for these chelates to be less stable than Gd-DTPA.[36,43] This can also be explained by the fact that amide groups coordinate to the gadolinium ion less strongly than carboxylate functions. There is, however, an exception when bulky substituents are present on the amide groups. This is notably the case for Gd-DTPA-BBMA (Figure 5).

3.4. O–Functionalised Derivatives of Gd-DTPA

3.4.1. Gd-DTPA-Bis(ester)s

Two derivatives, Gd-DTPA-BME and Gd-DTPA-BbzE, have been studied.[60] Their structures and relaxometric parameters are described in Table 6, and their NMRD profiles are presented in Figure 6. These compounds were obtained from DTPA-bis(anhydride) by reaction with the corresponding alcohol. Gd-DTPA-mono- and bis(propyl ester) were previously described by Sherry.[61]

The analysis of the data in Table 6 and their comparison with the data in Table 1 (for the parent compound Gd-DTPA) show that those two chelates have properties very similar to those of Gd-DTPA.

3.4.2. A Particular Case: One Additional Carboxylate Function on the Skeleton of Gd-DTPA

The synthesis of DTPA derivatives substituted at the alpha position of the central carboxyl group was described by Williams et al.[62] Amedio et al. reported the synthesis of (*S*)-N_6-carboxy-DTPA ester from L-aspartic acid.[63] In this work, Gd-(*S*)-N_6-carboxy-DTPA was synthesised (see Scheme 8 for the synthesis of the ligand). As a first step, ethanolamine is dialkylated with butyl bromoacetate. This intermediate is converted to its halogenated equivalent with *N*-bromosuccinimide to give compound **b**. At the same

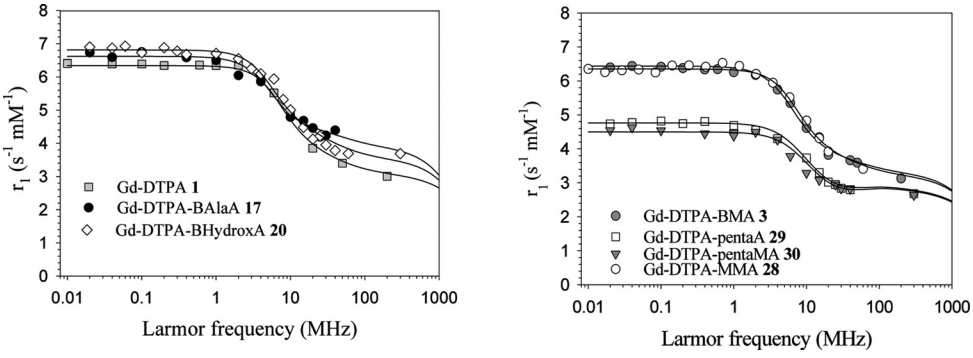

Figure 4. ^1H NMRD curves of water solutions of some *N*-functionalised derivatives of Gd-DTPA (T = 310 K). The lines correspond to the theoretical fittings of the data points by using the classical outer sphere and inner sphere theories. The curve for Gd-DTPA was added for comparison.

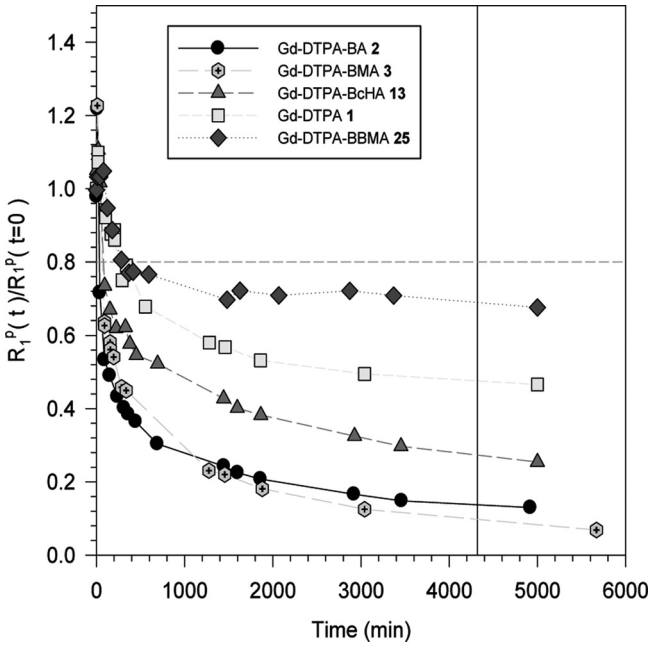

Figure 5. Evolution of the normalised water paramagnetic relaxation rate $R_1^P(t)/R_1^P(t = 0)$ with time for some *N*-functionalised derivatives of Gd-DTPA. The curve for Gd-DTPA was added for comparison (T = 37 °C, B = 0.47 T). The vertical line aims to show the ratio $R_1^P(t)/R_1^P(0)$ after 4320 min (which corresponds to three days), while the horizontal line aims to highlight the time required to reach 80 percent of the initial R_1^P value [$R_1^P(t)/R_1^P(0) = 0.8$].

Table 6. Structural and relaxometric parameters of two Gd-DTPA-bis(ester)s.

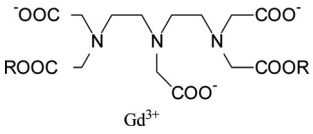

Compounds	r_1^{310} at 20 MHz (s^{-1} mM^{-1})	τ_M^{310}[a] (ns)	τ_R^{310} (ps)	τ_{S0}^{310} (ps)	τ_V^{310} (ps)
Gd-DTPA-BME **31** (R = CH_3)	3.6	150	66	82	15
Gd-DTPA-BBzE **32** (R = benzyl)	3.8	114	66[b]	79	16

[a] τ_M was measured independently by ^{17}O NMR spectroscopy. [b] For this compound, τ_R was measured independently by ^2H NMR spectroscopy; for the other, it was determined from the fitting of the NMRD curves.

time, L-aspartic acid is transformed into its ethyl or dibenzyl ester to increase the solubility in apolar media (compounds **c** and **d**, respectively). Intermediates **e** and **f** are then obtained by the reaction between compounds **b** and **c** or **b** and **d**, respectively, and are purified by chromatography on silica. (*S*)-N_6-carboxy-DTPA (**h**) is obtained by simple cleavage of ester **e** in acidic medium. The benzyl ester, compound **g**, could theoretically be obtained by selective cleavage of the *tert*-butyl ester in hydrochloric acid at 25 °C, but a mixture of compounds **f** and **g** (which is partially hydrolysed) was obtained. This mixture was therefore subjected

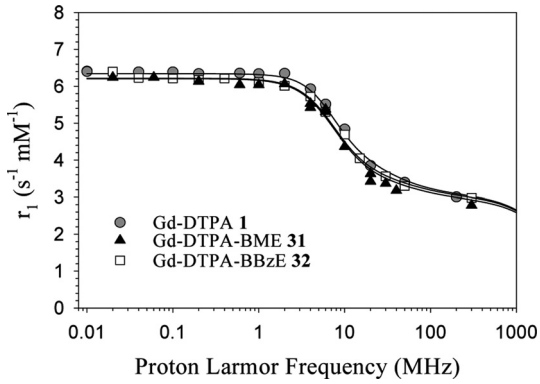

Figure 6. NMRD profiles of water solutions of Gd-DTPA-BME and Gd-DTPA-BbzE (T = 310 K). The curve for Gd-DTPA was added for comparison. The lines correspond to the theoretical fittings of the data points by using the classical outer sphere and inner sphere theories.

to catalytic hydrogenation to obtain compound **h**. The relaxometric properties of Gd-(*S*)-N_6-carboxy-DTPA are displayed in Table 7.

The relaxivity obtained is higher than that of Gd-DTPA, which shows that the presence of an additional coordinating group (the carboxylate function) does not prevent the access of one water molecule into the inner sphere of the gadolinium complex. On the contrary, the steric hindrance caused by the presence of the substituent favours the exchange of this coordinated water molecule and is thus responsible for a large decrease in the water residence time τ_M. The slight increase in τ_R with respect to that of Gd-DTPA is responsible for the observed higher relaxivity.

3.5. C-Functionalised Derivatives of Gd-DTPA

3.5.1. Benzyl Derivatives of Gd-DTPA

A benzyl group was grafted at different positions of the skeleton of DTPA to study the most judicious place to obtain the best efficiency of the contrast agent (Scheme 9).[64] The synthetic scheme used to produce these four compounds is described below.

3.5.1.1. The C_2-DTPA Derivative

Two methods have been proposed for the insertion of a benzyl group in position 2 (derivative **34**). The first one consists of reductive amination with an α-ketoacid (Scheme 10). This was described by Westerberg for the synthesis of a *p*-nitrobenzyl derivative.[65] The first three steps consist of a selective alkylation of the central amine. The next reductive amination in the presence of $NaBH_3CN$ is slow and appears to be the limiting step. The monosubstituted product is then alkylated with bromoacetic acid and deprotected under strongly alkaline conditions. The global yield of this tedious synthesis is about 4%.

The second method consists of the formation of a carbanion at the alpha position of one of the four carboxylic lateral groups of a DTPA pentaester and the subsequent

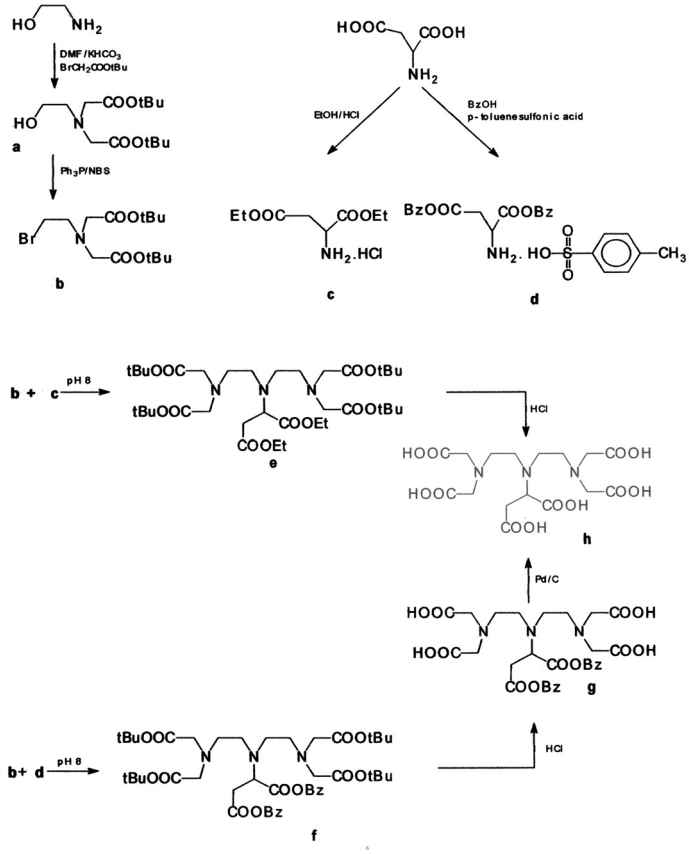

Scheme 8. Synthesis of (*S*)-N_6-carboxy-DTPA.

Table 7. Structural and relaxometric parameters of Gd-(*S*)-N_6-carboxy-DTPA.

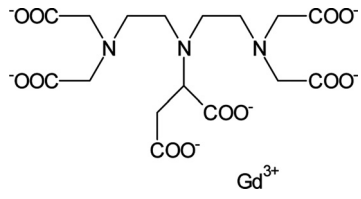

Compound	r_1^{310}[a] (s^{-1} mM^{-1})	τ_M^{310}[b] (ns)	τ_R^{310}[b] (ps)	τ_{S0}^{310} (ps)	τ_V^{310} (ps)
Gd-(*S*)-N_6-carboxy-DTPA **33**	4.8	32	73	164	41

[a] At 20 MHz. [b] For this compound, τ_M was measured independently by ^{17}O NMR spectroscopy, but τ_R was determined from the fitting of the NMRD curves.

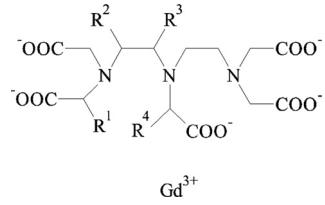

Scheme 9. Structures of four derivatives of Gd-DTPA, in which a benzyl group (Bz) has been grafted at different positions: Gd-(*R*,*S*)-C_2-Bz-DTPA (R^1 = Bz, R^2 = R^3 = R^4 = H) **34**, Gd-(*S*)-C_4-Bz-DTPA (R^2 = Bz, R^1 = R^3 = R^4 = H) **35**, Gd-(*S*)-N_6-(CHBzCOO$^-$)-DTPA (R^4 = Bz, R^1 = R^2 = R^3 = H) **36**, Gd-(*S*)-C_5-Bz-DTPA (R^3 = Bz, R^1 = R^2 = R^4 = H) **37**.

electrophilic attack of a halide derivative (Scheme 11). This four-step synthesis is rapid and has the advantage of starting from DTPA, thus avoiding the difficulties inherent in polyamine monoalkylation. The carbanion is obtained in situ at very low temperature and reacts with the benzyl cation. In all protocols,[66,67] a monosubstitution at position 2 was observed, but the amounts of the unreacted pentaester and polyalkylation were not negligible. The optimal conditions were obtained with an excess of potassium hexamethyldisilazane (KHMDS) and benzyl bromide in the presence of hexamethylphosphoramide (HMPA).

3.5.1.2. The C_4-DTPA Derivative

(*S*)-C_4-Bz-DTPA was synthesised as described by Brechbiel et al.[68] The commercially available amino acid is esterified, and the resulting ester hydrochloride is treated with EtN_3 and ethylenediamine to yield the corresponding amide. After reduction with an excess of borane, the crude triamine is purified by recrystallisation from MeOH. The polyaminocarboxylate ligand is then obtained by alkylation with *tert*-butyl bromoacetate in DMF and subsequent hydrolysis of the pentaester (Scheme 12).

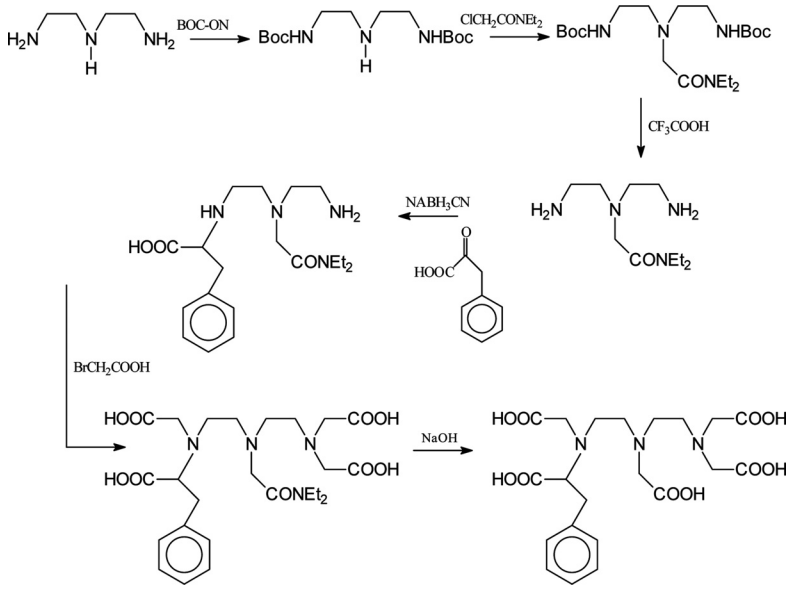

Scheme 10. Synthesis of (*R*,*S*)-C_2-Bz-DTPA by reductive amination.

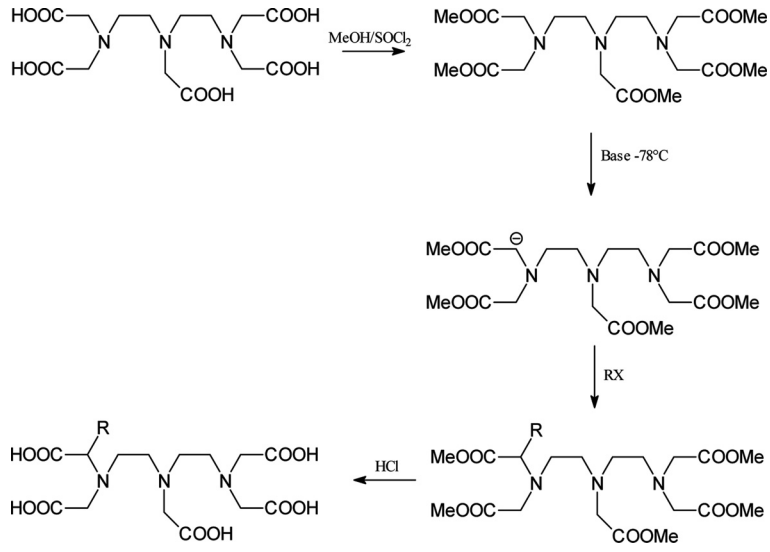

Scheme 11. Synthesis of (*R*,*S*)-C_2-Bz-DTPA by the formation of a carbanion (R = Bz).

3.5.1.3. The N_6-(CHBzCOO$^-$)-DTPA Derivative

The synthesis of Gd-(*S*)-N_6-(CHBzCOO$^-$)-DTPA (derivative **36**) was reported previously by Williams (see Scheme 13).[62]

3.5.1.4. The C_5-DTPA Derivative

The synthesis of DTPA substituted in position 5 (derivative **37**) was described by Brechbiel et al.[69] A dipeptide obtained by reaction between phenylalanylamide and *N*-hydroxy BOC glycine is transformed in a substituted derivative of diethylenetriamine. This intermediate is then reduced with borane and purified by precipitation as the hydrochlorate. The alkylation of the (*S*)-3-benzyl-diethylenetriamine gives the pentaester, which is hydrolysed with hydrochloric acid to form (*S*)-C_5-Bz-DTPA (Scheme 14).

These four compounds were characterised in water by their relaxometric properties, and their stability was compared with respect to zinc transmetallation. The results obtained are summarised in Table 8, in which they are compared according to their relaxometric parameters and their stability with respect to zinc transmetallation in order to evaluate the possible influence of the position of the benzyl substituent on those parameters.

The theoretical fitting of the reduced transverse relaxation rates of ^{17}O gives values of the water residence time τ_M ranging from 86 to 143 ns at 310 K; therefore, this parameter does not limit proton relaxivity at body temperature. The measured τ_M values are different for the four isomers: the DTPA derivatives substituted at the C-4 position or on the central arm indeed exhibit a faster water exchange than those substituted at the C-2 and C-5 positions. This

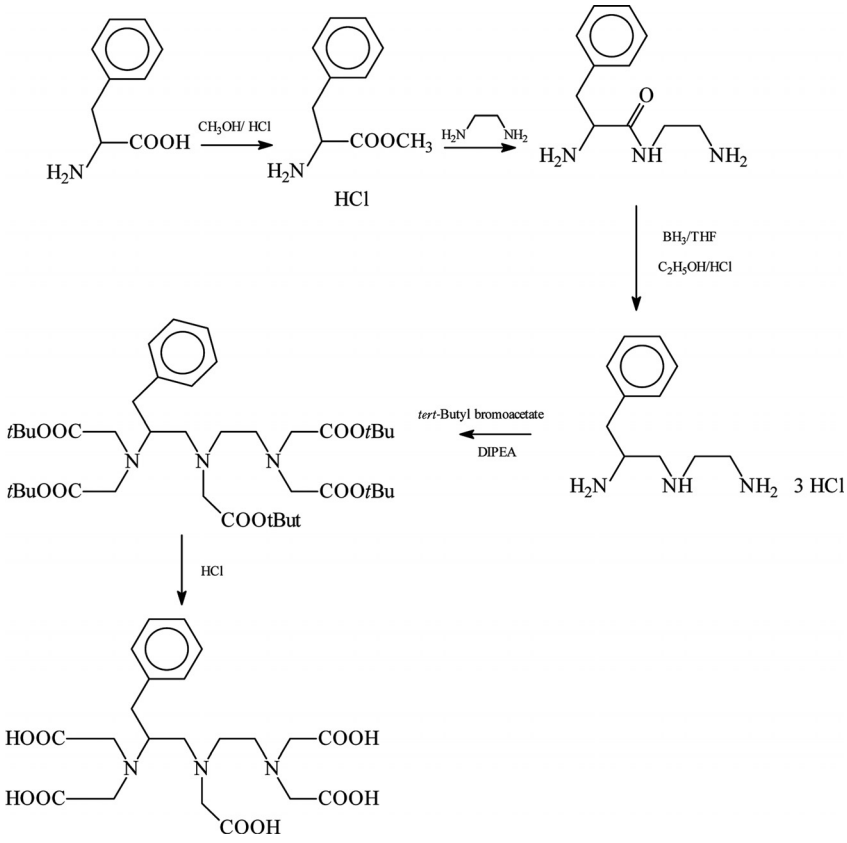

Scheme 12. Synthesis of (*S*)-C_4-Bz-DTPA.

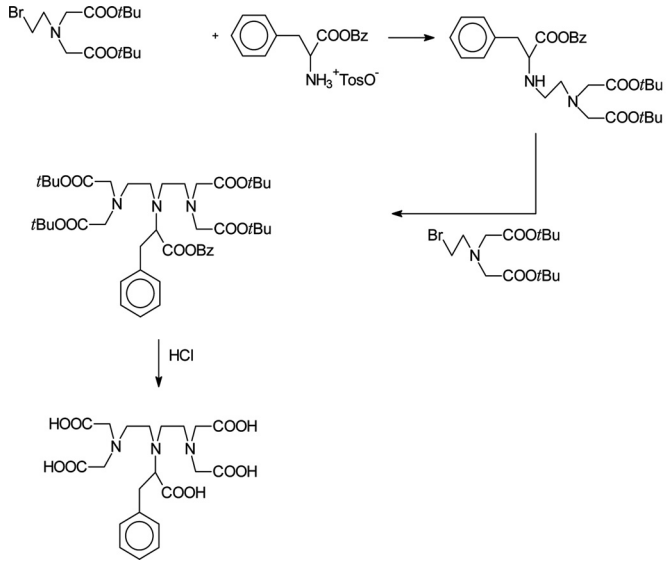

Scheme 13. Synthesis of N_6-(CHBzCOO$^-$)-DTPA.

suggests, therefore, that the steric hindrance induced by the substituent depends on its position on the DTPA skeleton. Depending on its proximity to the coordinated water molecule, the substituent can indeed accelerate the water exchange rate to a greater or lesser extent. It is worth noting that, in the case of derivative **34**, the measured τ_M is also influenced by the concentration of the two enantiomers, which are likely to be characterised by different exchange rates.

^{1}H-NMRD profiles show that the relaxivities of all *C*-substituted compounds (r_1 = 4.3–5.1 s^{-1} mM^{-1} at 20 MHz and 310 K) are higher than that of the parent Gd-DTPA. This is mainly due to the increase in the rotational correlation time τ_R, which is directly related to the molecular

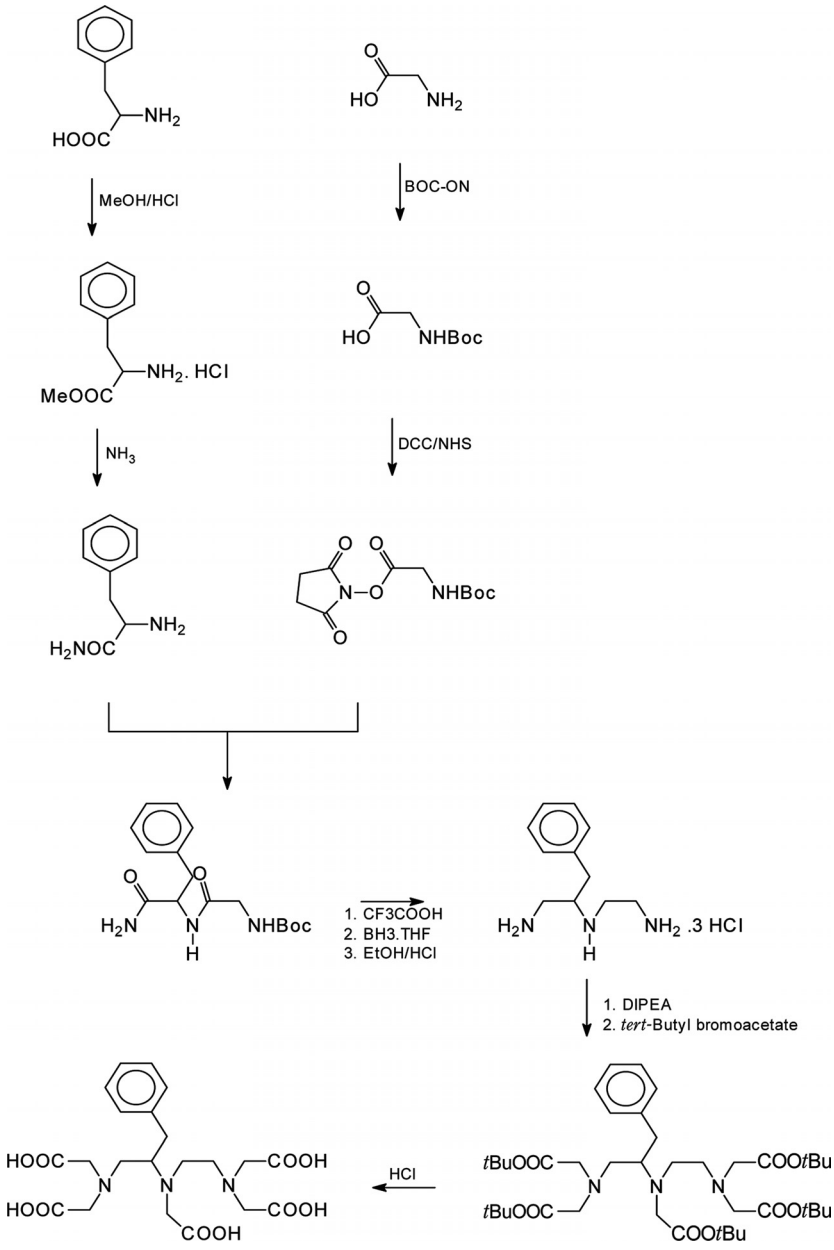

Scheme 14. Synthesis of C_5-Bz-DTPA.

mass of the chelate. The slight decrease in *r*, the proton–metal distance, which was observed for these *C*-functionalised chelates, can also explain the increase in their relaxivity.

Finally, the transmetallation assessment demonstrates that the *C*-substituted compounds are more stable than Gd-DTPA with the exception of Gd-N_6-(CHBzCOO$^-$)-DTPA. The highest stability with respect to transmetallation is achieved for the C_2, C_4 and C_5 derivatives. Apparently, the steric hindrance induced by the substituent at the C-2, C-4 or C-5 positions has a favourable effect by reducing the accessibility of the zinc ions.

Considering the practical aspects of the syntheses, which are not favourable for the C_5 derivative, the C-4 position seems thus to be preferable to link the Gd-DTPA moiety to a macromolecule or a specific vector in order to produce specific contrast agents of higher relaxivity and selectivity.

In this work, various C_4 derivatives of Gd-DTPA are thus investigated.

3.5.2. The C_4 Derivatives of Gd-DTPA

A series of C_4 derivatives of Gd-DTPA have been synthesised with a yield varying between 3 and 13%. Most of these compounds were prepared by using the same synthesis procedure as that for (*S*)-C_4-Bz-DTPA (Scheme 12), from the corresponding amino acid: alanine for Gd-(*S*)-C_4-Me-DTPA, valine for Gd-(*S*)-C_4-*i*Prop-DTPA, 2-aminoisobutyric acid for Gd-C_4-DiMe-DTPA, norleucine for Gd-(*S*)-C_4-*n*But-DTPA, leucine for Gd-(*S*)-C_4-*i*But-DTPA, 4-nitrophenylalanine for Gd-(*S*)-C_4-NO_2Bz-DTPA, 4-amino-

Table 8. Relaxometric parameters at 310 K of four derivatives of DTPA substituted with a benzyl group at four different positions.

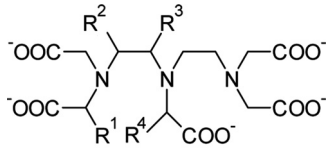

Gd^{3+}

Compounds	r_1^{310} at 20 MHz (s^{-1} mM^{-1})	τ_M^{310}[a] (ns)	τ_R^{310} (ps)	τ_{S0}^{310} (ps)	τ_V^{310} (ps)	Transmetallation[c] (%)
Gd-(*R*,*S*)-C_2-Bz-DTPA **34**	4.3	143	72[b]	87	16	36
Gd-(*S*)-C_4-Bz-DTPA **35**	4.8	87	62[b]	77	14	27
Gd-(*S*)-N_6-(CHBzCOO-)-DTPA **36**	5.1	87	68[b]	86	27	72
Gd-(*S*)-C_5-Bz-DTPA **37**	4.6	122	68	90	19	24

[a] τ_M was measured independently by ^{17}O NMR spectroscopy. [b] For these three compounds, τ_R was measured by ^2H NMR spectroscopy, whereas for the last one, it was determined from the fitting of the NMRD curves. [c] Percentage of transmetallated gadolinium complex after 4500 min.

phenylalanine for Gd-(*S*)-C_4-NH_2Bz-DTPA, serine for Gd-(*R*,*S*)-C_4-HM-DTPA and tryptophan for Gd-(*S*)-CH_2In-DTPA.[70,71] Gd-(*S*)-C_4-PheNHCS-NHBz-DTPA (derivative **47**) was obtained from the reaction between C_4-aminobenzyl-DTPA and phenyl-isothiocyanate.[72] Finally, the three last compounds, Gd-C_4-benzyl-4-aminosal-DTPA, Gd-C_4-benzyl-5-aminosal-DTPA and Gd-C_4-benzylisothioureyl-GGE3-DTPA were obtained from isothiocyanatobenzyl-DTPA (Scheme 15).[73]

Gd-C_4-Benzylisothioureyl-GGE3-DTPA, for which a peptide containing six amino acids is grafted on the skeleton of DTPA, aims to target apoptotic cells. This peptide (E3), for which the sequence from the N-terminal extremity is Thr-Leu-Val-Ser-Ser-Leu, was selected by the phage display technique. This gadolinium chelate was studied in the apoptotic liver cells of mice by MRI.[74] The relaxometric properties of these compounds are summarised in Table 9.

The data show that all of these chelates have a similar or higher relaxivity than Gd-DTPA. This increase in relaxivity can be explained by an increase in τ_R due to an increase in the molecular size of the complex. To illustrate this, the NMRD profiles of some of the derivatives are presented in Figure 7.

The data also show a reduction of τ_M for all the Gd-C_4-DTPA derivatives (τ_M^{310} varies between 57 and 110 ns) as compared to Gd-DTPA (τ_M^{310} = 143 ns). The coordinated water exchange rate increases at 310 K by 30 to 90% for the gadolinium chelates. These results thus confirm that a judicious substitution on the DTPA skeleton allows an acceleration of the coordinated water exchange rate.[75] This has also been reported previously for some other derivatives of Gd-DTPA, like MS-325,[7] Gd-(*S*)-EOB-DTPA[6] and MP-2269.[76] This observation is useful for the design of macromolecular or vectorised contrast agents for molecular imaging.

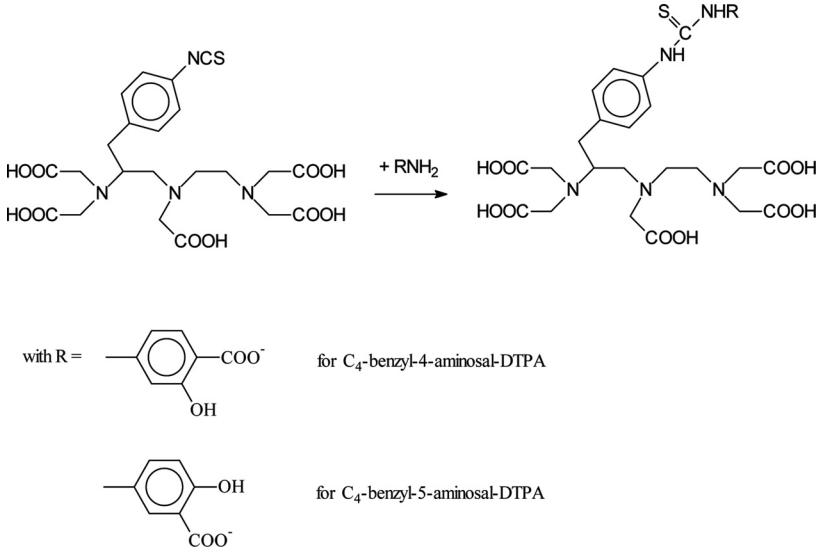

Scheme 15. Synthesis of C_4-benzyl-4-aminosal-DTPA **48**, C_4-benzyl-5-aminosal-DTPA **49** and C_4-benzylisothioureyl-GGE3-DTPA **50**.

Table 9. Relaxometric properties at 310 K of various C_4 derivatives of Gd-DTPA.

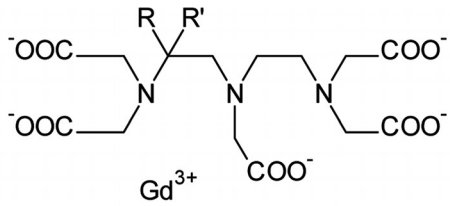

Compounds	R_1^{310} at 20 MHz (s^{-1} mM^{-1})	τ_M^{310} (ns)[a]	τ_R^{310} (ps)	τ_{S0}^{310} (ps)	τ_V^{310} (ps)
Gd-(*S*)-C_4-Me-DTPA **38** (R = CH_3; R' = H)	3.8	91	57	88	20
Gd-(*S*)-C_4-iProp-DTPA **39** [R = $CH(CH_3)_2$; R' = H]	4.3	98	68	96	20
Gd-C_4-DiMe-DTPA **40** (R = R' = CH_3)	4.1	57	60	97	20
Gd-(*S*)-C_4-*n*Bu-DTPA **41** [R = $(CH_2)_3CH_3$; R' = H]	4.5	82	71	87	22
Gd-(*S*)-C_4-*i*Bu-DTPA **42** [R = $CH_2CH(CH_3)_2$; R' = H]	4.2-4.3	80	61[b]	96	15
Gd-(*S*)-C_4-NO_2Bz-DTPA **43** (R = 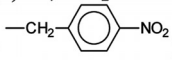 ; R' = H)	6.2	94	78[b]	108	30
Gd-(*S*)-C_4-NH_2Bz-DTPA **44** (R = 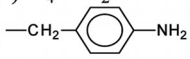 ; R' = H)	6.0	88	73[b]	73	21
Gd-(*R*,*S*)-C_4-HM-DTPA **45** (R = CH_2OH; R' = H)	4.5	89	53[b]	87	20
Gd-(*S*)-CH_2In-DTPA **46** (R = 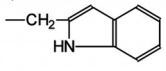 ; R' = H)	5.5	71	75[b]	117	24
Gd-(*S*)-C_4-PheNHCS-NHBz-DTPA **47** (R = 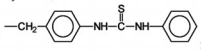 ; R' = H)	7.05	110	105	58	27
Gd-C_4-benzyl-4-aminosal-DTPA **48** (see Figure 21 for R; R' = H)	5.25	82	88	83	27
Gd-C_4-benzyl-5-aminosal-DTPA **49** (see Figure 21 for R; R' = H)	5.27	64	86	82	27
Gd-C_4-benzylisothioureyl-GGE3-DTPA **50** (see Figure 21 for R; R' = H)	5.10	80	103	84	25

[a] τ_M was measured independently by ^{17}O NMR spectroscopy. [b] For these compounds, τ_R was measured by ^2H NMR spectroscopy, whereas for the others, it was determined from the fitting of the NMRD curves.

Regarding zinc transmetallation, the C_4-monosubstituted derivatives are more stable than Gd-DTPA. As explained above, this can be explained by the steric hindrance induced by the substituent, which reduces the accessibility of the zinc ions. As an example, the transmetallation curves of three characteristic C_4 derivatives of Gd-DTPA are presented in Figure 8.

3.6. The C_4-Functionalised DTPA-Bis(amide)s

Two derivatives, Gd-(*S*)-Bz-DTPA-BMA and Gd-(*S*)-EOB-DTPA-BMA (Scheme 16), were synthesised by a classical scheme starting from the corresponding C_4 derivative of DTPA. This pentacarboxylated compound was treated with acetic anhydride in the presence of pyridine to produce the C_4-functionalised DTPA-bis(anhydride).[77] The subsequent amination was carried out with an excess of methylamine (Scheme 17).

For the two C_4-functionalised DTPA-BMA derivatives, the residence time of the water molecule in the first coordi-

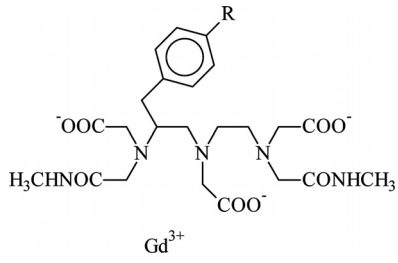

Scheme 16. Structures of C_4-functionalised DTPA-BMA compounds. R = H for Gd-(*S*)-Bz-DTPA-BMA and R = OC_2H_5 for Gd-(*S*)-EOB-DTPA-BMA.

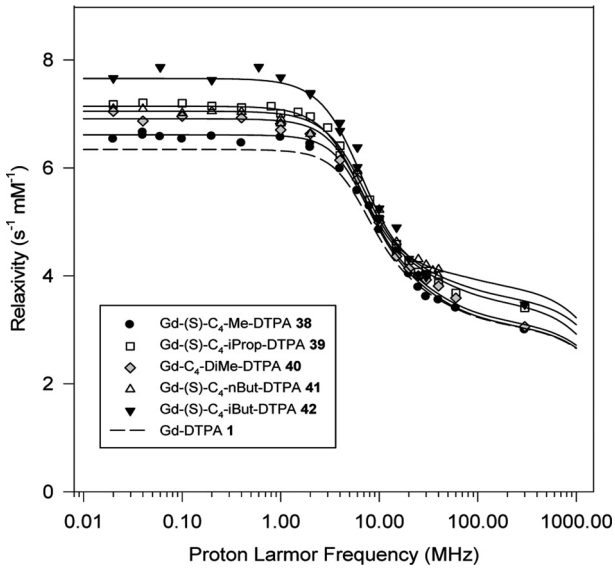

Figure 7. NMRD profiles at 310 K of various C_4 derivatives of Gd-DTPA. The solid lines correspond to the theoretical fittings of the data points by using the classical outer sphere and inner sphere theories. The curve for Gd-DTPA (dashed line) was added for comparison.

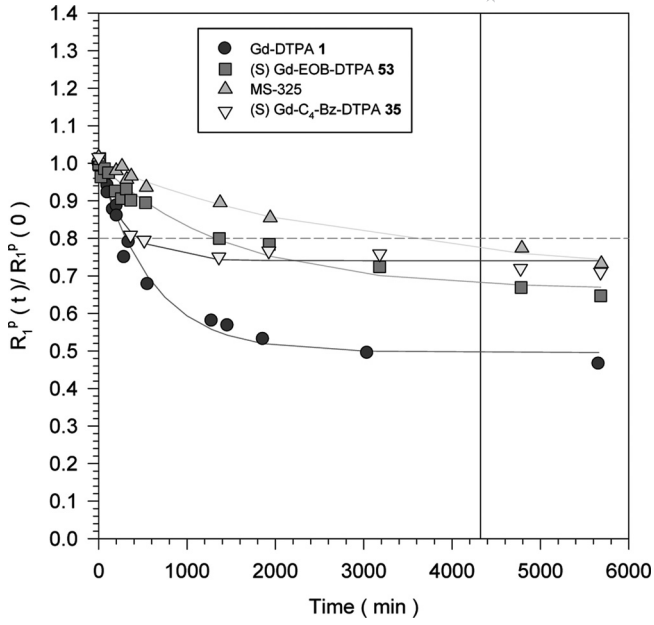

Figure 8. Evolution of the normalised water paramagnetic relaxation rate $R_1^P(t)/R_1^P(t = 0)$ with time for (*S*)-Gd-EOB-DTPA (Eovist®, Bayer HealthCare, Germany) and (*S*)-Gd-C_4-Bz-DTPA. The curves for Gd-DTPA and MS-325, another C_4-functionalised derivative of Gd-DTPA, were added for comparison (T = 37 °C, B = 0.47 T). The vertical line aims to show the ratio $R_1^P(t)/R_1^P(0)$ after 4320 min (which corresponds to three days), while the horizontal line aims to highlight the time required to reach 80 percent of the initial R_1^P value [$R_1^P(t)/R_1^P(0) = 0.8$].

nation sphere of the gadolinium ion (τ_M) has an intermediate value between that of Gd-DTPA and that of Gd-DTPA-BMA (Table 10). These data thus tend to confirm the adverse effect of the presence of the amide functions on the value of τ_M and the beneficial effect of C_4 substitution on the reduction of that parameter. The increase in τ_M relative to the values obtained for the C_4 derivatives of Gd-DTPA [Gd-(*S*)-EOB-DTPA and Gd-(*S*)-C_4-Bz-DTPA] does not, however, affect the measured relaxivities. The parameter τ_M has indeed a small influence on the relaxivity of the small gadolinium complexes at 20 MHz, but it becomes a very critical parameter for the macromolecular ones.

As assessed by the Zn^{2+} transmetallation process, the C_4-functionalised DTPA-BMA compounds are less stable than Gd-DTPA and slightly more stable than Gd-DTPA-BMA.

In conclusion, although they are more difficult to synthesise than the *N*-functionalised derivatives of Gd-DTPA, the C_4 compounds are better suited for covalent binding to a

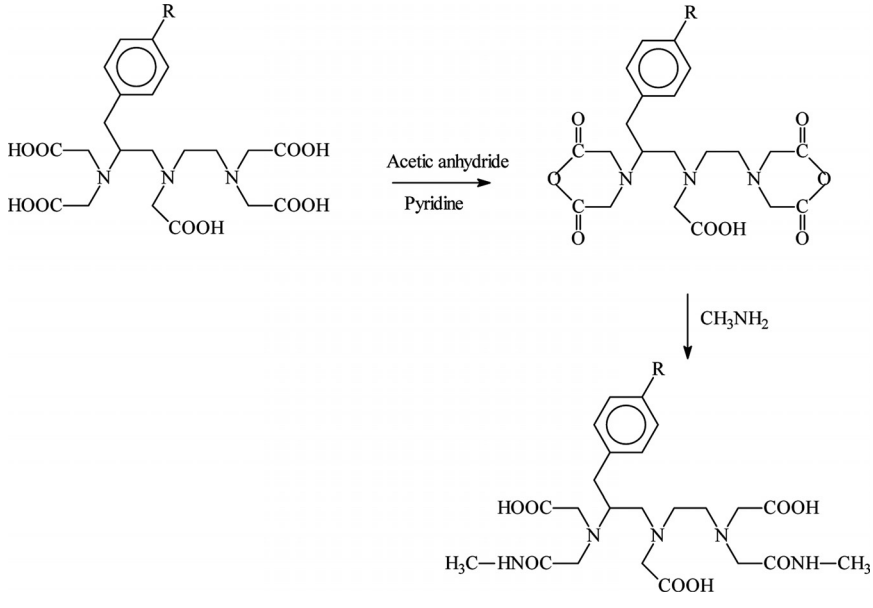

Scheme 17. Synthesis of C_4-functionalised DTPA-BMA.

Table 10. Relaxometric parameters at 310 K of two C_4-functionalised DTPA-BMA compounds. The parameters of the parent compounds Gd-DTPA, Gd-DTPA-BMA, Gd-(*S*)-EOB-DTPA and Gd-(*S*)-C_4-Bz-DTPA are added for comparison.

Compounds	r_1 at 20 MHz (s^{-1} mM^{-1})	τ_{S0} (ps)	τ_V (ps)	τ_R[a] (ps)	τ_M[b] (ns)	Transmetallation[c] (%)
Gd-(*S*)-EOB-DTPA-BMA **51** (R = OC_2H_5)	5.2	67	15	61	472	87
Gd-(*S*)-Bz-DTPA-BMA **52** (R = H)	4.7	72	15	63	435	78
Gd-DTPA **1**	3.8	82	23	59	143	51
Gd-DTPA-BMA **2**	3.8	84	16	69	967	91
Gd-(*S*)-EOB-DTPA **53** (R = OC_2H_5)	5.5	69	17	61	82	31
Gd-(*S*)-C_4-Bz-DTPA **35**	4.8	81	17	61	87	27

[a] τ_R was measured independently by ^{2}H NMR spectroscopy. [b] τ_M was measured independently by ^{17}O NMR spectroscopy. [c] Percentage of transmetallated gadolinium chelate after 4500 min.

macromolecule or to a specific vector in the context of the design of new specific contrast agents for molecular imaging.

4. Current and Further Developments in Obtaining Gadolinium Complexes of Higher Relaxivity

4.1. Macromolecular Contrast Agents

4.1.1. Covalently Bound Conjugates

To increase the relaxivity of the paramagnetic contrast agents, intense research has been carried out in the covalent coupling of contrast agents with macromolecules like polymers, dendrimers, proteins, and so on. The large molecular size of such adducts indeed allows a slowing down of the molecular motion, thus resulting in higher values of the rotational correlation time τ_R as compared with those of the small gadolinium complexes. This should cause a large increase in the relaxivity of the contrast agents, provided that the other parameters influencing the water relaxation rate are in an optimal range. Up to now, most of the applications involving macromolecular contrast agents have exploited their prolonged intravascular lifetime as opposed to the small gadolinium chelates, which rapidly equilibrate between the plasma and the extravascular interstitial space.

To design such macromolecular adducts, a compromise must be found between the size of the macromolecule, which has to allow a complete elimination of the contrast agent by glomerular filtration, and a good tolerability in the body. Thus, they have to be biocompatible and kinetically stable.

The most studied macromolecules are proteins. Several ways have been investigated to conjugate small gadolinium chelates with the amine functions of proteins: DTPA-bis(anhydride) as the acylating agent,[78–80] a mixed anhydride of DTPA,[81,82] an *N*-hydroxysuccinic ester,[83] squaric acid esters as a linker[84,85] or isothiocyanatobenzyl groups.[86] The most studied system is represented by human serum albumin (HSA) labelled with Gd-DTPA.[87] Aime et al.[88] have studied the frequency and temperature dependence of proton and ^{17}O relaxivities of $(Gd\text{-}DTPA)_{45}$-HSA. The observed behaviour is typical of systems whose relaxivity is limited by a long residence time by the coordinated water molecule.[89] Sieving et al.[81] have synthesised a poly(L-lysine) containing 60 to 90 chelating groups (DTPA or DOTA) per molecule. Once complexed with Gd^{III} ions, the paramagnetic chains were conjugated to HSA. The relatively small relaxation enhancement shown by these gadolinium complexes when bound to polylysine is accounted for by the high internal mobility of the paramagnetic moieties.[21] An analogous result was observed by using the squaric acid unit as a linker between the macromolecule and the Gd chelates.[90] Labelling monoclonal antibodies with Gd-DTPA has also been considered for targeting tumours.[91,92]

The grafting of small gadolinium complexes to polymers was also extensively investigated. Derivatives of Gd-DTPA complexes or Gd-DOTA complexes were grafted onto poly(L-lysine).[93,94] Curtet et al. studied Gd-polylysine chelates coupled with a monoclonal antibody targeting the carcinoma of the colon.[91] The coupling was achieved without important loss of immunoreactivity, and the targeting allows a relaxation rate increase of approximately 20%. Poly(L-lysine)-DTPA was also grafted to PEG in order to increase the relaxivity.[95] Other studies have explored the possibility of attaching Gd complexes as side chains to a linear synthetic polymer chain[96–99] or, alternatively, to incorporate the Gd chelate into the polymer chain itself.[32] The relaxivities of those macromolecular adducts have, however, been found to be lower than expected. This was explained by the highly flexible nature of the macromolecule. Higher efficiency was obtained with Gd-DTPA-bis(amide) alkyl copolymers $[(Gd\text{-}DTPA\text{-}BA)\text{-}(CH_2)_n]_x$ (n = 6, 10 or 12).[33] Relaxivity studies indicated that Gd polyaspartamide complexes containing sulfadiazine groups also possess relaxivities higher than that of Gd-DTPA.[100]

The use of polysaccharide to increase the molecular weight of the contrast agent was also explored. For example, dextran containing a spacer arm was grafted onto gadolinium chelates.[101] The advantage of dextran is its high capacity for functionalisation with different types of bonds, like carbamate, epichlorhydrine, periodate or carboxymethyl.[102–109] Several Gd chelates were also grafted on inulin.[110,111]

Table 11. Properties of some gadolinium chelates interacting noncovalently with human serum albumin (HSA). The water proton relaxation rates (B_0 = 20 MHz) measured in a solution of the chelate in 4% HSA at T = 310 K (if not indicated otherwise), as well as their association constant K_a with HSA are presented. N corresponds to the associated number of binding sites. K_a was measured by the proton relaxometry technique (T = 310 K if not indicated otherwise).[88]

Gd chelate	R_1^P (s^{-1} mM^{-1})	K_a (M^{-1})	Reference
(*S*)-Gd-EOB-DTPA	12.6 [Gd chelate] = 1 mM	7.7×10^2 (N = 1)	[6,130]
(*R*)-Gd-EOB-DTPA	8.8 [Gd chelate] = 1 mM	1.8×10^2 (N = 1)	[130]
MS-325	26.7 [Gd chelate] = 1 mM	6.1×10^3 (N = 1)	[7,131]
MP2269	30.9 [Gd chelate] = 1 mM	1.6×10^4 (N = 1–2)	[132]
Gd-BOPTA	16 [Gd chelate] = 1 mM	1.5×10^3 (N = 1)	[133]
Gd-DTPA-$(BOM)_2$		3.6×10^3 (N = 1)	[88]
Gd-DTPA-$(BOM)_3$	48 [Gd chelate] = 1 mM (T = 298 K)	4.0×10^4 (N = 1) (T = 298 K)	[88,134]
Gd-DTPA-IOP	12.9 [Gd chelate] = 1 mM (T = 312 K)	3.8×10^2 (N = 1)	[135]
Gd-DTPA-IOPsp	18.4 [Gd chelate] = 1 mM (T = 312 K)	4.8×10^3 (N = 1)	[135]
$(Gd\text{-}DTPA)_2$bis(indole)	13.5 [Gd^{3+}] = 1 mM	1.0×10^4 (N = 1)	[136]
DTPA *N*-functionalised by $CH_2P(O)(OH)CH_2NBn_2$	18 [Gd chelate] = 0.8 mM	4.5×10^3 (N = 1)	[137]
Gd-C_2-Bz-DTPA	13 [Gd chelate] = 1 mM	1.3×10^3 (N = 1)	[132]
Gd-C_4-sulfaphenazol-DTPA	24.6 [Gd chelate] = 1 mM	$K_{a1} = 7.5\times10^5$ (N = 1) $K_{a2} = 2\times10^4$ (N = 2)	[138] [138]
Gd-C_4-thyroxin-DTPA	36.1 [Gd chelate] = 1 mM	1.0×10^4 (N = 2)	[139]

The clinical application of Gd chelates grafted onto polymers is limited by the slow excretion of the complexes and thus the accumulation of the toxic gadolinium ion. To avoid this problem, biodegradable polydisulfide macromolecular complexes were prepared. Wen et al.[112] synthesised and characterised poly(glutamic acid) Gd chelates as biodegradable blood pool compounds. These are based on the disulfide–thiol exchange to allow degradation of the macromolecules by the endogenous thiol and thus facilitate the excretion of the Gd chelate.[113,114] Another biodegradable macromolecular chelate, a Gd-DTPA cystine copolymer, was grafted with PEG of different sizes to modify its physicochemical properties, in order to enhance the in vivo MRI contrast of these agents, and to study the effect of the PEG chain length (MW = 550, 1000 and 2000) on these properties.[115] PEG 2000 showed the most prominent enhancement in the blood pool for a longer period of time.

Gd complexes have also been grafted on PAMAM dendrimers.[116–128] An increase in the relaxivity was observed, which can be explained by the steric hindrance that predominates at the periphery and produces an increase in the τ_R value. MRI studies have shown that dendritic Gd chelates containing pyridoxamine groups enhance the contrast of the MR images of the liver, provide prolonged intravascular lifetime and produce highly contrasted visualisation of the blood vessels.[129]

Globally, for all these macromolecular adducts, the increase in the relaxivity is not as large as predicted by theory. This can be mainly attributed to the local rotational mobility of the gadolinium chelate when it is grafted onto the macromolecule.

4.1.2. Noncovalent Conjugates

Several research groups have studied noncovalent complexes, where the gadolinium chelate equilibrates between a free state and a state bound to a macromolecule. This strategy enables a rapid elimination of the contrast agent by the kidneys and consequently reduces its toxicity.

Most of the studies have concerned human serum albumin (HSA), which is by far the most abundant endogenous macromolecule. These gadolinium complexes are summarised in Table 11 and Scheme 18.

A lot of derivatives of Gd-DOTA interacting noncovalently with HSA were also designed, and they are characterised by relaxivities similar to those of the above derivatives.[135,140,141]

4.2. Lipophilic Contrast Agents

All Gd-DTPA derivatives cited before are water-soluble and can be administered to the patient by intravenous injection. When the complexes are insoluble in water, they are studied in different formulations like liposomes or mixed micelles.

The introduction of aliphatic chains on DTPA increases its lipophilic character. Some lipophilic complexes (Scheme 19) were synthesised by reaction of DTPA-bis(anhydride) with the appropriate amine. Some monoamide derivatives were also prepared as described by Anelli (Scheme 20).[142]

Mixed micelles are prepared by mixing the lipophilic Gd complex with a phospholipid bearing a chain of 16 carbon atoms and a surfactant (like Tween 80). Several formulations of mixed micelles have been investigated for imaging the cardiovascular system.[143] This kind of system has been characterised by measuring the mean diameter of the micelles [with the photon correlation spectroscopy (PCS) technique] and by recording the NMRD profiles.[144,145] Typical NMRD profiles of paramagnetic micelles with a mean diameter of 20 nm are shown in Figure 9. The relaxometric parameters characterising these lipophilic derivatives of Gd-DTPA incorporated in mixed micelles are presented in Tables 12 and 13.

The observed decrease in the relaxivity for Gd-DTPA-$BC_{18}A$ can be explained by an increase in the flexibility of

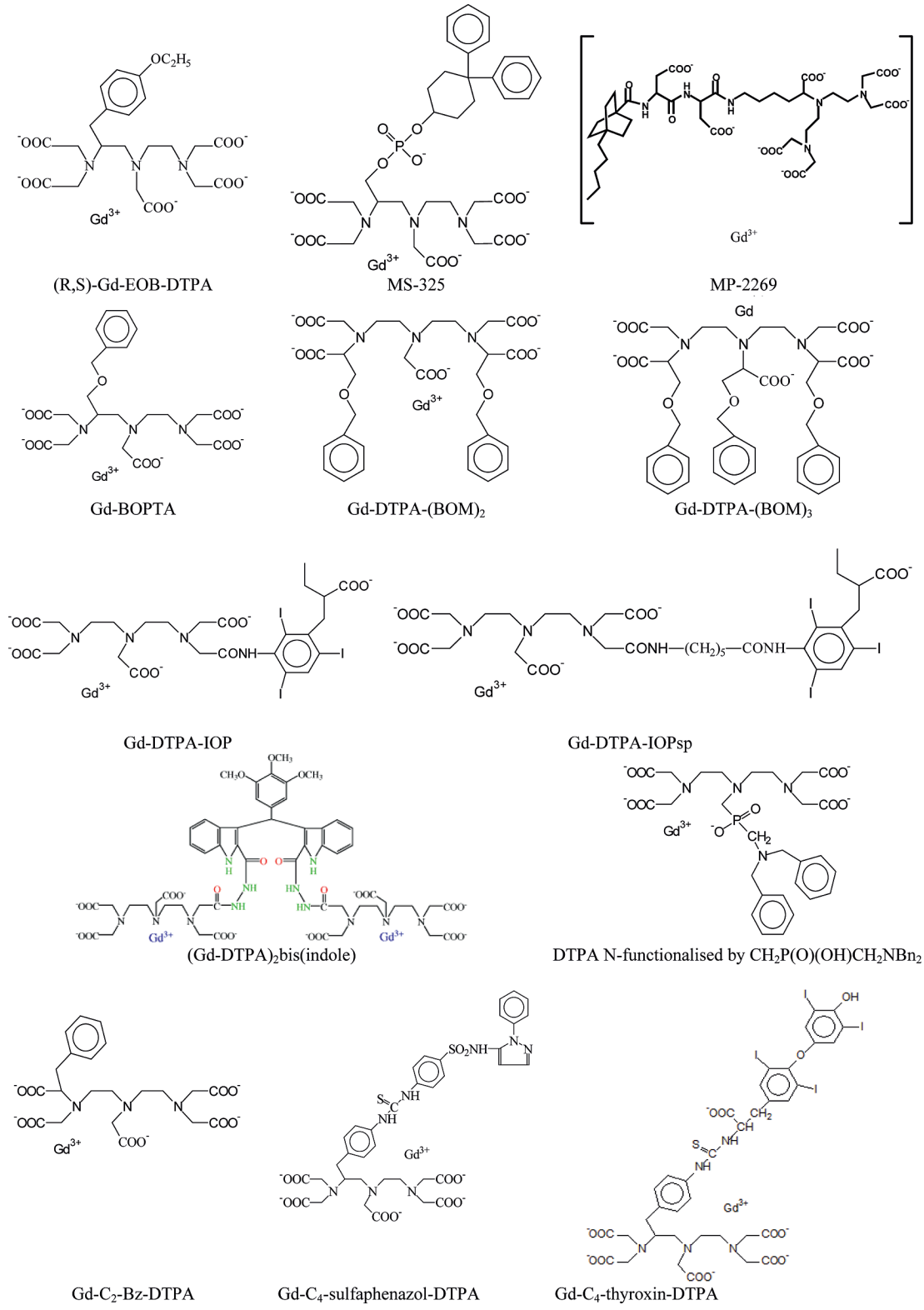

Scheme 18. Structures of the gadolinium complexes described in Table 11.

the complex due to its alkyl chains, which are longer than those of the used phospholipid.

For the liposome formulations, the Gd complex was mixed with DPPC (dipalmitoylphosphatidylcholine). The mixture was then sonicated and extruded to obtain monodisperse samples. The relaxometric properties of these paramagnetic liposomes are shown in Figure 10 and Table 14. Paramagnetic liposomes are rapidly taken up by cells of the reticuloendothelial system and they are used to target the liver and spleen.[146,147]

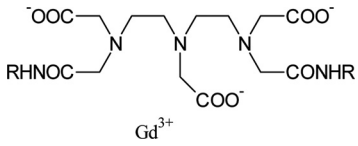

Scheme 19. Structures of some lipophilic bis(amide) derivatives of Gd-DTPA (with R = $C_{12}H_{25}$, $C_{14}H_{29}$, $C_{16}H_{33}$, $C_{18}H_{37}$, $C_{18}H_{35}$, LDP).

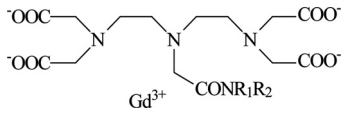

Scheme 20. Structure of some lipophilic monoamide derivatives of Gd-DTPA (with R^1 = H, R^2 = $C_{12}H_{25}$, $C_{14}H_{29}$, $C_{16}H_{33}$, $C_{18}H_{37}$, $C_{18}H_{35}$, LDP).

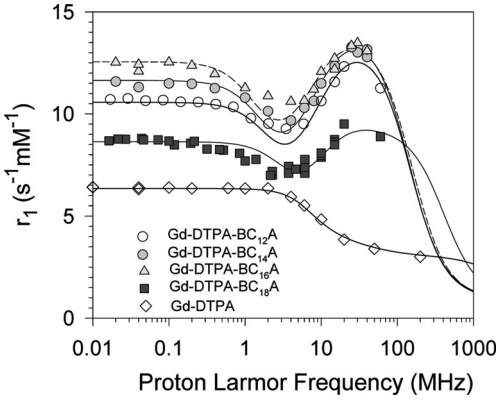

Figure 9. NMRD profiles of some paramagnetic micelles for which the length of the lipophilic chain grafted on Gd-DTPA is varied. The NMRD profile of Gd-DTPA was added for comparison.

Table 12. Relaxometric parameters at 310 K of lipophilic bis(amide) derivatives of Gd-DTPA incorporated into mixed micelles.

Compounds	r_1[a] (s^{-1} mM^{-1})	τ_R (ns)	τ_M (μs)	τ_{S0} (ps)	τ_V (ps)
Gd-DTPA-B(LDP)A	12.2	2.06	1.67	176	30
Gd-DTPA-BC_{12}A	12.5	3.09	1.38	160	30
Gd-DTPA-BC_{14}A[b]	12.9	3.05	1.30	175	30
Gd-DTPA-BC_{16}A[b]	13.0	2.97	1.28	209	30
Gd-DTPA-BC_{18}A[b]	8.0	0.62	1.47	101	27

[a] At 20 MHz. [b] Ref.[144]

Table 13. Relaxometric parameters at 310 K of lipophilic monoamide derivatives of Gd-DTPA incorporated into mixed micelles.

Compounds	r_1[a] (s^{-1} mM^{-1})	τ_R (ns)	τ_M (μs)	τ_{S0} (ps)	τ_V (ps)
Gd-DTPA-MLDP	13.7	1.28	1.14	170	30
Gd-DTPA-MC_{14}A[b]	14.2	0.91	0.68	194	41
Gd-DTPA-MC_{16}A[b]	16.7	1.12	0.51	154	39
Gd-DTPA-MC_{18}A[b]	17.2	1.07	0.50	127	38

[a] At 20 MHz. [b] Ref.[145]

The relaxivity at 20 MHz reaches a minimum for the derivatives with a chain length of 12 or 14 carbon atoms, which matches the chain length of the main component of the liposome. This can be explained by an increased immobilisation of the Gd complex inside the liposome and a decreased global water exchange rate through the bilayer membrane. On the other hand, the relaxivity of Gd-DTPA-BC_{18}Ai, which is characterised by a double bond in its alkyl chains, is higher than that of the other derivatives. Thus, it seems that the presence of the double bond in the alkyl chains of the Gd complex is beneficial because of an increase in the water exchange rate through the bilayer.[152–153]

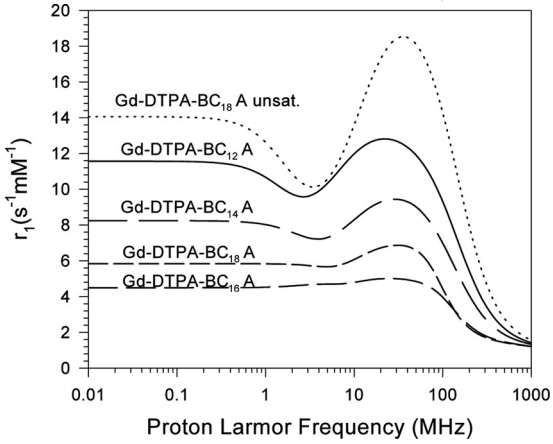

Figure 10. NMRD profiles of liposomal solutions of derivatives of Gd-DTPA bearing a lipophilic chain of different lengths.[148,149]

Table 14. Relaxometric parameters at 310 K of some lipophilic bis(amide) derivatives of Gd-DTPA incorporated into liposomes.

Compound	r_1[a] (s^{-1} mM^{-1})	τ_R (ns)	τ_M (μs)	τ_{S0} (ps)	τ_V (ps)
Gd-DTPA-BC_{12}A	12.7	3.4	1.4	199	36
Gd-DTPA-BC_{14}A	9.69	5.4	2.1	112	30
Gd-DTPA-BC_{16}A	5.1	19.7	4.4	42	28
Gd-DTPA-BC_{18}A	6.8	22.0	3.5	63	27
Gd-DTPA-BC_{18}Ai	16.7	1.9	0.7	173	28

[a] At 20 MHz.

Amphiphilic Gd-DTPA-bis(amide)s containing long-chain phenylalanine esters were incorporated into liposomes.[150] The derivative bearing a chain of 14 carbon atoms has shown the highest relaxivity, because its alkyl chain length matches those of DPPC phospholipids.

Recently, paramagnetic liposomes made of Gd-DMPE-DTPA (dimyristoyl-sn-*glycero*-3-phosphoethanolamine-DTPA) with a PEG coating have been used for the detection of solid tumours.[151] Lattuada et al. have prepared a Gd-DTPA-cholesterol complex as an MRI agent.[152]

Strijkers et al. studied the relaxation properties of paramagnetic liposomes as a function of composition, temperature and magnetic field. PEGylated liposomes with a diameter of approximately 100 nm were designed to favour the pharmacokinetic properties in vivo. The relaxivity of liposomes with unsaturated DOPC phospholipids was higher than those of liposomes with saturated DSPC lipids. Addition of cholesterol was essential to obtain monodisperse liposomes and led to a further increase in relaxivity, but the relaxivity was limited by water exchange through the bilayer.[153]

Another kind of paramagnetic liposome can be prepared by encapsulation of hydrophilic Gd-DTPA. Recently, Lo-

kling et al. have used paramagnetic pH-sensitive liposomes for monitoring pathological changes in pH by MRI. These liposomes are stable and release the encapsulated Gd complex when exposed to lower pH in a target tissue.[154,155] Paramagnetic thermosensitive liposomes can also been designed.[156] They are composed of a Gd or Mn compound enclosed by a phospholipid membrane with a distinct gel-to-liquid crystalline phase-transition temperature. The phospholipid membrane changes from a gel phase to a liquid phase, which is associated with an increased transmembrane permeability. Under these conditions, the paramagnetic liposomes demonstrate a significant increase in their relaxivity, which can be attributed to the increased water exchange rate between the interior and the exterior spaces.[157]

All these examples show the same tendency for the development of new MRI contrast agents: the production of macromolecular or nanoparticulate agents bearing several Gd complexes in order to obtain a higher relaxivity than that of the single chelate. This strategy utilises the increase in the rotational correlation time, τ_R, when the Gd complex is bound to the macromolecular carrier. Nevertheless, this is not always as efficient as expected, not only because of the local mobility of the Gd complex, but also because the coordinated water exchange rate is not always optimised, especially when amide bonds are used to link the Gd chelate to the macromolecule. In the case of the Gd complexes incorporated into the liposomal cavity, the relaxivity is also limited by the water exchange rate through the bilayer. Thus, the development of new efficient contrast agents first requires tuning the structure of the chelate to optimise its water exchange rate and secondly avoiding local mobility of the Gd complex in the macromolecular adduct to allow a high increase in the rotational correlation time.

5. Conclusions

This work discusses the synthesis and relaxometric properties of different gadolinium complexes, mostly derived from Gd-DTPA, as well as the wide range of chemical and biological applications that exist for MRI contrast agents. In summary, the following conclusions can be highlighted: to optimise the structure of Gd complexes for molecular imaging, the vector should be grafted on C_4-DTPA derivatives rather than amide or ester derivatives of Gd-DTPA. C_4-DTPA derivatives are more stable (from the thermodynamic and kinetic point of view) than the parent compound, and their efficiency is higher.

Contrast-agent-enhanced MRI is an invaluable tool for the diagnosis of cancer and many other diseases; it is currently used more and more frequently for molecular imaging of experimental animals. With improved targeted delivery of these agents, the diagnosis of specific diseases will become more sensitive, accurate and ultimately simpler. Finally, smart agents, which respond to biological phenomena by altering the intensity of signal enhancement in a conditional fashion, are steps towards unravelling the complex connectivity of developmental biological systems. Furthermore, these agents could represent the prelude to complete and noninvasive medical examinations that are safe, fast and accurate.

Acknowledgments

The authors thank the Center for Microscopy and Molecular Imaging (CMMI), supported by the European Regional Development Fund and the Walloon Region. This work was supported by the Biomed II MACE Programme of the Commission of the European Communities (contract BMH4-CT-96–0051; DG12-SSMA), the French Community of Belgium (ARC Programmes 95/00–194, 00/05–258 and 05/10–335) and the Fond National de la Recherche Scientifique (FNRS). The support and concerted sponsorship of COST Action D38 and the EMIL Programme are kindly acknowledged.

[1] H. Schmitt-Willich, M. Brehm, Ch. L. J. Ewers, G. Michl, A. Muller-Fahrnow, O. Petrov, J. Platzek, B. Raduchel, D. Sulzle, *Inorg. Chem.* **1999**, *38*, 1134–1144.
[2] F. Uggeri, S. Aime, P. Anelli, M. Botta, M. Brochetta, C. de Haen, G. Ermondi, M. Grandi, P. Paoli, *Inorg. Chem.* **1995**, *34*, 633–642.
[3] P. F. Sieving, A. D. Watson, S. M. Rocklage, *Bioconjugate Chem.* **1990**, *1*, 65–71.
[4] R. Rebizak, M. Schaefer, E. Dellachevies, *Bioconjugate Chem.* **1997**, *8*, 605–610.
[5] D. Shahbazi-Gahrouei, M. Williams, S. Rizvi, B. J. Allen, *J. Magn. Reson. Imaging* **2001**, *14*, 169–174.
[6] L. Vander Elst, F. Maton, S. Laurent, F. Seghi, F. Chapelle, R. N. Muller, *Magn. Reson. Med.* **1997**, *38*, 604–614.
[7] R. N. Muller, B. Raduchel, S. Laurent, J. Platzek, C. Piérart, P. Mareski, L. Vander Elst, *Eur. J. Inorg. Chem.* **1999**, 1949–1955.
[8] K. Adzamli, L. Vander Elst, S. Laurent, R. N. Muller, *Magn. Reson. Mater. Phys., Biol. Med.* **2001**, *12*, 92–95.
[9] L. Vander Elst, M. Port, I. Raynal, C. Simonot, R. N. Muller, *Eur. J. Inorg. Chem.* **2003**, 2495–2501.
[10] L. Vander Elst, I. Raynal, M. Port, P. Tisnès, R. N. Muller, *Eur. J. Inorg. Chem.* **2005**, 1142–1148.
[11] S. Liu, D. S. Edwards, *Bioconjugate Chem.* **2001**, *12*, 630–634.
[12] I. Virgolini, P. Angelberger, S. Li, Q. Yang, A. Kurtaran, M. Raderer, N. Neuhold, K. Kaserer, M. Leimer, M. Peck-Radosavljevic, W. Scheithauer, B. Niederle, H.-G. Eichler, P. Valent, *Eur. J. Nucl. Med.* **1996**, *23*, 1388–1399.
[13] C. J. Mathias, D. Hubers, P. S. Low, M. A. Green, *Bioconjugate Chem.* **2000**, *11*, 253–257.
[14] A. D. Nunn, K. E. Linder, M. F. Tweedle, *Q. J. Nucl. Med.* **1997**, *41*, 155–162.
[15] a) P. Caravan, J. J. Ellison, T. J. Mc Murry, R. B. Lauffer, *Chem. Rev.* **1999**, *99*, 2293–2352; b) R. B. Lauffer, *Chem. Rev.* **1987**, *87*, 901–927.
[16] C. F. G. C. Geraldes, S. Laurent, *Contrast Med. Mol. Imaging* **2009**, *4*, 1–23.
[17] S. Aime, D. Delli Castelli, S. Geninatti Crich, E. Gianolio, E. Terreno, *Acc. Chem. Res.* **2009**, *42*, 822–831.
[18] C. S. Bonnet, E. Tóth, *Future Med. Chem.* **2010**, *2*, 367–384.
[19] S. Laurent, L. Vander Elst, R. N. Muller, *Contrast Med. Mol. Imaging* **2006**, *1*, 128–137.
[20] E. Brucher, A. D. Sherry in *The Chemistry of Contrast Agents in Medical Magnetic Resonance Imaging* (Eds.: A. E. Merbach, E. Toth), John Wiley & Sons, Chichester, **2001**, ch. 6, pp. 243–279.

[21] a) N. R. Puttagunta, W. A. Gibby, V. L. Puttagunta, *Invest. Radiol.* **1996**, *31*, 619–624; b) N. R. Puttagunta, W. A. Gibby, V. L. Puttagunta, *Invest. Radiol.* **1996**, *31*, 739–742.

[22] C. Corot, J.-M. Idee, A.-M. Hentsch, R. Santus, C. Mallet, V. Goulas, B. Bonnemain, D. Meyer, *J. Magn. Reson. Imag.* **1998**, *8*, 695–702.

[23] C. Corot, A.-M. Hentsch, L. Curtelin, *Invest. Radiol.* **1994**, *29 (Suppl. 2)*, S164–S167.

[24] M. F. Tweedle, J. J. Hagan, K. Kumar, S. Mantha, C. A. Chang, *Magn. Reson. Imaging* **1991**, *9*, 409–415.

[25] S. Laurent, L. Vander Elst, R. N. Muller in *Encyclopedia of Magnetic Resonance* (Eds.: R. K. Harris, R. Wasylishen), Wiley, Chichester, **2009**, DOI: 10.1002/9780470034590.emrstm1049.

[26] a) M. Botta, *Eur. J. Inorg. Chem.* **2000**, 399–407; b) D. A. Fulton, E. M. Elemento, S. Aime, L. Chaabane, M. Botta, D. Parker, *Chem. Commun.* **2006**, 1064–1066 ; c) C. S. Bonnet, P. H. Fries, S. Crouzy, O. Sénèque, F. Cisnetti, D. Boturyn, P. Dumy, P. Delangle, *Chem. Eur. J.* **2009**, *15*, 7083–7093 ; d) C. S. Bonnet, P. H. Fries, S. Crouzy, P. Delangle, *J. Phys. Chem. B* **2010**, *114*, 8770–8781.

[27] a) I. Solomon, *Phys. Rev.* **1955**, *99*, 559–565; b) N. Bloembergen, *J. Chem. Phys.* **1957**, *27*, 572–573.

[28] J. H. Freed, *J. Chem. Phys.* **1978**, *68*, 4034–1037.

[29] J. W. Chen, R. L. Belford, R. B. Clarkson, *J. Phys. Chem. A* **1998**, *102*, 2117–2130.

[30] a) A. Beeby, I. M. Clarkson, R. S. Dickins, S. Faulkner, D. Parker, L. Royle, A. S. de Sousa, J. A. G. Williams, M. Woods, *J. Chem. Soc. Perkin Trans. 2* **1999**, 493–503; b) W. D. Horrocks, D. R. Sudnick, *Acc. Chem. Res.* **1981**, *14*, 384–392; c) I. Nasso, C. Galaup, F. Havas, P. Tisnes, C. Picard, S. Laurent, L. Vander Elst, R. N. Muller, *Inorg. Chem.* **2005**, *44*, 8293–8305; d) N. Geum, I. Nasso, B. Mestre, P. Tisnès, C. Picard, S. Laurent, R. N. Muller, L. Vander Elst, *Bioorg. Med. Chem. Lett.* **2006**, *16*, 5309–5312; e) S. Laurent, L. Vander Elst, C. Galaup, R. N. Muller, C. Picard, *Bioorg. Med. Chem. Lett.* **2007**, *17*, 6230–6233.

[31] a) J. A. Peters, J. Huskens, D. J. Raber, *Prog. Nucl. Magn. Reson. Spectrosc.* **1996**, *28*, 283–350; b) S. Laurent, L. Vander Elst, M. Wautier, C. Galaup, R. N. Muller, C. Picard, *Biorg. Med. Chem. Lett.* **2007**, *14*, 6230–6233.

[32] T. J. Swift, R. E. Connick, *J. Chem. Phys.* **1962**, *37*, 307–320.

[33] K. Micskei, L. Helm, E. Brücher, A. E. Merbach, *Inorg. Chem.* **1993**, *32*, 3844–3850.

[34] S. Laurent, L. Vander Elst, F. Botteman, R. N. Muller, *Eur. J. Inorg. Chem.* **2008**, *28*, 4369–4379.

[35] K. Micskei, D. H. Powell, L. Helm, E. Brücher, A. E. Merbach, *Magn. Reson. Chem.* **1993**, *31*, 1011–1020.

[36] a) S. Aime, M. Botta, M. Fasano, E. Terreno, *Acc. Chem. Res.* **1999**, *32*, 941–949; b) S. Zhang, K. Wu, A. D. Sherry, *Invest. Radiol.* **2001**, *36*, 82–86.

[37] E. Toth, I. Van Uffelen, L. Helm, A. E. Merbach, D. Ladd, K. Briley-Saebo, K. E. Kellar, *Magn. Reson. Chem.* **1998**, *36*, S125–S134.

[38] E. Toth, L. Helm, K. E. Kellar, M. E. Merbach, *Chem. Eur. J.* **1999**, *5*, 1202–1211.

[39] E. Toth, D. Pubanz, S. Vauthey, L. Helm, A. E. Merbach, *Chem. Eur. J.* **1996**, *2*, 1607–1615.

[40] A. Barge, G. Cravotto, E. Gianolio, F. Fedeli, *Contrast Med. Mol. Imaging* **2006**, *1*, 184–188.

[41] R. N. Muller, D. Declercq, P. Vallet, F. Giberto, B. Daminet, H. W. Fischer, F. Maton, Y. Van Haverbeke, *Proc. ESMRMB, 7th Annual Congress*, Strasbourg, **1990**, p. 394.

[42] P. Vallet, *Relaxivity of Nitroxide Stable Free Radicals. Evaluations by Field Cycling Method and Optimisation*, Ph. D. Thesis, University of Mons-Hainaut, Belgium, **1992**.

[43] S. Laurent, L. Vander Elst, F. Copoix, R. N. Muller, *Invest. Radiol.* **2001**, *36*, 115–122.

[44] W. C. Eckelman, S. M. Karesh, R. C. Reba, *J. Pharm. Sci.* **1975**, *64*, 704–706.

[45] S. Aime, M. Botta, W. Dastru, M. Fasano, M. Panero, A. Arnelli, *Inorg. Chem.* **1993**, *32*, 2068–2071.

[46] C. Gèze, C. Mouro, F. Hindré, M. Le Plouzennec, C. Moinet, R. Rolland, L. Alderighi, A. Vacca, G. Simonneaux, *Bull. Soc. Chim. Fr.* **1996**, *133*, 267–272.

[47] C. F. G. C. Geraldes, A. M. Urbano, M. C. Alpoim, A. D. Sherry, K.-T. Kuan, R. Rajagopalan, F. Maton, R. N. Muller, *Magn. Reson. Imaging* **1995**, *13*, 401–420.

[48] H. Lammers, F. Maton, D. Pubanz, M. W. van Laren, H. van Bekkum, A. E. Merbach, R. N. Muller, J. A. Peters, *Inorg. Chem.* **1997**, *36*, 2527–2532.

[49] F. Botteman, G. Nicolle, L. Vander Elst, S. Laurent, A. E. Merbach, R. N. Muller, *Eur. J. Inorg. Chem.* **2002**, 2686–2693.

[50] F. Botteman, *Synthesis and Characterization of Gd-DTPA Bisamide Derivatives*, Master Thesis, UMH, University of Mons-Hainaut, Belgium, **1997**.

[51] C. Burtéa, S. Laurent, S. Lecocq, L. Vander Elst, R. N. Muller, *19th Annual Meeting of the European Society for Magnetic Resonance in Medicine and Biology*, Cannes, France, **2002**.

[52] S. Laurent, L. Vander Elst, Y. Fu, R. N. Muller, *Bioconjugate Chem.* **2004**, *15*, 99–103.

[53] S. Boutry, C. Burtea, S. Laurent, L. Vander Elst, R. N. Muller, *Magn. Reson. Med.* **2005**, *53*, 800–807.

[54] P. R. Selvin, J. Jancarik, M. Li, L.-W. Hung, *Inorg. Chem.* **1995**, *34*, 700–705.

[55] P. L. Anelli, L. Calabi, C. de Haen, F. Fedeli, P. Losi, M. Murru, F. Uggeri, *Gazz. Chim. Ital.* **1996**, *126*, 89–97.

[56] E. Krejcarek, K. L. Tucker, *Biochem. Biophys. Res. Commun.* **1977**, *77*, 581–585.

[57] Y. Arano, T. Uezono, H. Akizawa, M. Ono, K. Wakisaka, M. Nakayama, H. Sakahara, J. Konishi, A. Yokoyama, *J. Med. Chem.* **1996**, *39*, 3451–3460.

[58] S. Aime, M. Botta, M. Fasano, S. Paoletti, L. Anelli, F. Uggeri, M. Virtuani, *Inorg. Chem.* **1994**, *33*, 4707–4711.

[59] S. Aime, A. Barge, J. I. Bruce, M. Botta, J. A. K. Howard, J. M. Moloney, D. Parker, A. S. de Sousa, M. Woods, *J. Am. Chem. Soc.* **1999**, *121*, 5762–5771.

[60] S. Laurent, L. Vander Elst, F. Botteman, R. N. Muller, *Eur. J. Inorg. Chem.* **2008**, *28*, 4369–4379.

[61] A. D. Sherry, W. P. Cacheris, K.-T. Kuan, *Magn. Reson. Med.* **1988**, *8*, 180–190.

[62] M. A. Williams, H. Rapoport, *J. Org. Chem.* **1993**, *58*, 1151–1158.

[63] J. C. Amedio, G. Van Wagenen, G. Zavlin, *Synth. Commun.* **2000**, *30*, 3755–3763.

[64] S. Laurent, F. Botteman, L. Vander Elst, R. N. Muller, *Helv. Chim. Acta* **2004**, *87*, 1077–1089.

[65] D. A. Westerberg, P. L. Carney, P. E. Rogers, S. J. Kline, D. K. Johnson, *J. Med. Chem.* **1989**, *32*, 236–243.

[66] J. F. W. Keana, J. S. Mann, *J. Org. Chem.* **1990**, *55*, 2868–2871.

[67] H. Nemoto, J. Cai, H. Nakamura, M. Fujiwara, Y. Yamamoto, *J. Organomet. Chem.* **1999**, *581*, 170–175.

[68] M. W. Brechbiel, O. A. Gansow, R. W. Atcher, J. Schlom, J. Esteban, D. E. Simpson, D. Colcher, *Inorg. Chem.* **1986**, *25*, 2772–2781.

[69] M. W. Brechbiel, O. A. Gansow, *Bioconjugate Chem.* **1991**, *2*, 187–194.

[70] K. Bernard, *Synthèse et étude de la mobilité moléculaire de dérivés de l'acide diéthylènetriaminepentaacétique (DTPA)*, Master Thesis, UMH, University of Mons-Hainaut, Belgium, **1998**.

[71] V. Jourquin, *Influence de la substitution sur la relaxivité paramagnétique des complexes du gadolinium. Synthèse et étude de dérivés C_4 substitués du Gd-DTPA*, Master Thesis, UMH, University of Mons-Hainaut, Belgium, **1999**.

[72] N. Guerit, *Synthèse de dérivés C-benzylés et C-phénylés de l'acide diéthylènetriamine pentaacétique (DTPA). Etude des interactions non-covalentes avec l'albumine sérique humaine*, Master Thesis, UMH, University of Mons-Hainaut, Belgium, **1998**.

[73] C. Henoumont, *Etude par diffusométrie RMN des interactions non covalentes de molécules avec des protéines*, Master Thesis, UMH, University of Mons-Hainaut, Belgium, **2004**.
[74] C. Laumonier, *Molecular Imaging: New Specific Peptides for Apoptosis Obtained by Phage Display*, Ph. D. Thesis, UMH University of Mons-Hainaut, Belgium, **2005**.
[75] S. Laurent, F. Botteman, L. Vander Elst, R. N. Muller, *Magn. Reson. Mater. Phys. Biol. Med.* **2004**, *16*, 235–245.
[76] E. Toth, F. Connac, L. Helm, K. Adzamli, A. E. Merbach, *J. Biol. Inorg. Chem.* **1998**, *3*, 606–613.
[77] S. Laurent, F. Botteman, L. Vander Elst, R. N. Muller, *Eur. J. Inorg. Chem.* **2004**, 463–468.
[78] D. J. Hnatowich, W. W. Layne, R. L. Childs, D. Laintegne, M. A. Davis, T. W. Griffin, P. W. Doherty, *Science* **1983**, *220*, 613–615.
[79] R. B. Lauffer, T. J. Brady, *Magn. Reson. Imaging* **1985**, *3*, 11–16.
[80] M. D. Ogan, U. Schmiedl, M. Moseley, W. Grodd, H. Paajanen, R. C. Brasch, *Invest. Radiol.* **1987**, *22*, 665–671.
[81] P. F. Sieving, A. D. Watson, S. M. Rocklage, *Bioconjugate Chem.* **1990**, *1*, 65–71.
[82] F. Maisano, L. Gozzini, C. de Haen, *Bioconjugate Chem.* **1992**, *3*, 212–217.
[83] M. Spanoghe, D. Lanens, R. Dommisse, A. van der Linden, F. Alderweireldt, *Magn. Reson. Imaging* **1992**, *10*, 913–917.
[84] L. F. Tietze, C. Schroter, S. Gabius, U. Brinck, A. Goerlach-Graw, J. H. Gabius, *Bioconjugate Chem.* **1991**, *2*, 48–53.
[85] S. Aime, M. Botta, S. Geninatti Crich, G. Giovenzana, G. Palmisano, M. Sisti, *Bioconjugate Chem.* **1999**, *10*, 192–199.
[86] P. Niemi, T. Reisto, I. Hemmilä, M. Kormano, *Invest. Radiol.* **1991**, *26*, 820–824.
[87] M. E. Mosseley, D. L. White, S. C. Wang, M. G. Wikstrrm, J. W. Dupon, G. Gobbel, K. Roth, R. C. Brasch, *J. Comput. Assist. Tomogr.* **1989**, *13*, 215–221.
[88] S. Aime, M. Fasano, E. Terreno, M. Botta in *The Chemistry of Contrast Agents in Medical Magnetic Resonance Imaging* (Eds.: A. E. Merbach, E. Toth), John Wiley & Sons, Chichester, **2001**, ch. 5, pp. 193–241.
[89] Y. Berthezène, V. Vexler, D. C. Price, J. Wisner-Dupon, M. E. Moseley, K. P. Aicher, R. C. Brasch, *Invest. Radiol.* **1992**, *27*, 346–351.
[90] S. Aime, M. Botta, S. Geninatti Crich, G. Giovenzana, G. Palmisano, M. Sisti, *Bioconjugate Chem.* **1999**, *10*, 192–199.
[91] C. Curtet, F. Maton, T. Havet, M. Slinkin, A. Mishra, J. F. Chatal, R. N. Muller, *Invest. Radiol.* **1998**, *33*, 752–761.
[92] C. Wu, W. Brechbiel, R. W. Kozak, O. A. Gansow, *Bioorg. Med. Chem. Lett.* **1994**, *4*, 449–454.
[93] V. S. Vexler, O. Clement, H. Schmitt-Willich, R. C. Brash, *J. Magn. Reson. Imaging* **1994**, *4*, 381–388.
[94] E. E. Uzgiris, H. Cline, B. Moasser, B. Grimmond, M. Amaratunga, J. F. Smith, G. Goddard, *Biomacromolecules* **2004**, *5*, 54–61.
[95] A. A. Bogdanov, R. Weissleder, H. W. Frank, A. V. Bogdanova, N. Nossif, B. K. Schaffer, E. Tsai, M. I. Papisov, T. J. Brady, *Radiology* **1993**, *87*, 701–706.
[96] P. F. Sieving, A. D. Watson, S. M. Rocklage, *Bioconjugate Chem.* **1990**, *1*, 65–71.
[97] G. Schuhmann-Giampieri, H. Schmitt-Willich, T. Frenzel, W. R. Press, H. J. Weinmann, *Invest. Radiol.* **1991**, *26*, 969–974.
[98] T. Desser, D. Rubin, H. Muller, F. Qing, S. Khodor, Y. Zanazzi, D. Wellons, K. Kellar, J. Toner, R. Snow, *J. Magn. Reson. Imaging* **1994**, *4*, 467–472.
[99] S. Aime, M. Botta, S. G. Crich, G. Giovenzana, G. Palmisano, M. Sisti, *Bioconjugate Chem.* **1999**, *10*, 192–199.
[100] G. P. Yan, M. L. Liu, L. Y. Li, *Bioconjugate Chem.* **2005**, *16*, 967–971.
[101] P. Rongved, B. Lindberg, J. Klaveness, *Carbohydr. Res.* **1991**, *214*, 315–323.
[102] S. W. A. Bligh, C. T. Harding, P. J. Sadler, R. A. Bulman, G. M. Bydder, J. M. Pennock, J. D. Kelly, I. A. Clatham, J. A. Marriott, *Magn. Reson. Med.* **1991**, *17*, 516–532.
[103] K. C. P. Li, R. G. Quisling, F. E. Armitage, D. Richardson, C. Mladinich, *Magn. Reson. Imaging* **1992**, *10*, 439–444.
[104] D. Meyer, M. Schaefer, A. Bouillot, S. Beauté, C. Chambron, *Invest. Radiol.* **1991**, *26 (Suppl. 1)*, S50–S52.
[105] D. Meyer, M. Schaefer, C. Chambon, S. Beauté, *Invest. Radiol.* **1994**, *29*, S90–S92.
[106] C. Corot, M. Schaefer, S. Beauté, P. Bourrinet, S. Zehaf, V. Benize, M. Sabatou, D. Meyer, *Acta Radiol.* **1997**, *412*, 91–99.
[107] C. Casali, M. Janier, E. Canet, J. F. Obadia, S. Benderbous, C. Corot, D. Revel, *Acad. Radiol.* **1998**, *5 (Suppl. 1)*, S214–S218.
[108] R. Rebizak, M. Schaefer, E. Dellacherie, *Eur. J. Pharm. Sci.* **1999**, *7*, 243–248.
[109] C. B. Sirlin, D. R. Vera, J. A. Corbeil, M. B. Caballero, R. B. Buxton, R. F. Mattrey, *Acad. Radiol.* **2004**, *11*, 1361–1369.
[110] P. Lebduskova, J. Kotek, P. Hermann, L. Vander Elst, R. N. Muller, I. Lukes, J. A. Peters, *Bioconjugate Chem.* **2004**, *15*, 881–889.
[111] L. Granato, S. Laurent, L. Vander Elst, K. Djanashvili, J. A. Peters, R. N. Muller, *Contrast Media Mol. Imaging* **2011**, *6*, 482–491.
[112] X. Wen, E. F. Jackson, R. E. Price, F. E. Kim, Q. Wu, S. Wallace, C. Charnsangavej, J. G. Gelovani, C. Li, *Bioconjugate Chem.* **2004**, *15*, 1408–1415.
[113] Y. Zong, X. Wang, K. C. Goodrich, A. M. Mohs, D. L. Parker, Z. R. Lu, *Magn. Reson. Med.* **2005**, *53*, 835–842.
[114] Z. R. Lu, D. L. Parker, K. C. Goodrich, X. Wang, J. G. Dalle, H. R. Buswell, *Magn. Reson. Med.* **2004**, *51*, 27–34.
[115] A. M. Mohs, Y. Zong, J. Guo, D. L. Parker, Z. R. Lu, *Biomacromolecules* **2005**, *6*, 2305–2311.
[116] E. C. Wiener, M. W. Brechbiel, H. Brothers, R. L. Magin, O. A. Gansow, D. A. Tomalia, P. C. Lauterbur, *Magn. Reson. Med.* **1994**, *31*, 1–8.
[117] S. Laus, A. Sour, R. Ruloff, E. Toth, A. E. Merbach, *Chem. Eur. J.* **2005**, *11*, 3064–3076.
[118] V. J. Venditto, C. A. Regino, M. W. Brechbiel, *Mol. Pharm.* **2005**, *2*, 302–311.
[119] S. J. Wang, M. Brechbiel, E. C. Wiener, *Invest. Radiol.* **2003**, *38*, 662–668.
[120] H. Kobayaski, S. Kawamoto, S. K. Jo, H. L. Bryant, M. W. Brechbiel, R. A. Star, *Bioconjugate Chem.* **2003**, *14*, 388–394.
[121] N. Sato, H. Kobayashi, A. Higara, T. Saga, K. Togashi, J. Konishi, M. W. Brechbiel, *Magn. Reson. Med.* **2001**, *46*, 1169–1173.
[122] H. Kobayaski, S. Kawamoto, T. Saga, N. Sato, A. Higara, T. Ishimori, J. Konishi, K. Togashi, M. W. Brechbiel, *Magn. Reson. Med.* **2001**, *46*, 781–788.
[123] H. Kobayaski, N. Sato, A. Higara, T. Saga, Y. Nakamoto, H. Ueda, J. Konishi, K. Togashi, M. W. Brechbiel, *Magn. Reson. Med.* **2001**, *45*, 454–460.
[124] H. Kobayaski, N. Sato, S. Kawamoto, T. Saga, A. Higara, T. L. Haque, T. Ishimori, J. Konishi, K. Togashi, M. W. Brechbiel, *Bioconjugate Chem.* **2001**, *12*, 100–107.
[125] L. H. Bryant, M. W. Brechbiel, C. Wu, J. W. Bulte, V. Herynek, J. A. Frank, *J. Magn. Reson. Imaging* **1999**, *9*, 348–352.
[126] L. D. Margerum, B. K. Campion, M. Koo, N. Shargill, J.-J. Lai, A. Marumoto, P. C. Sontum, *J. Alloys Compd.* **1997**, *249*, 185–190.
[127] J. Tacke, G. Adam, H. Claben, A. Muhler, A. Prescher, R. W. Gunther, *Magn. Reson. Imaging* **1997**, *7*, 678–682.
[128] H. C. Roberts, M. Saeed, T. P. L. Roberts, A. Muhler, D. M. Shames, J. S. Mann, M. Stiskal, F. Demsar, R. C. Brasch, *Magn. Reson. Imaging* **1997**, *7*, 331–338.
[129] G. P. Yan, B. Hu, M. L. Liu, L. Y. Li, *J. Pharm. Pharmacol.* **2005**, *57*, 351–357.

[130] L. Vander Elst, F. Capelle, S. Laurent, R. N. Muller, *J. Biol. Inorg. Chem.* **2001**, *6*, 196–200.
[131] P. Caravan, N. J. Cloutier, M. T. Greenfield, S. A. McDermid, S. U. Dunham, J. W. Bulté, J. C. Amedio, R. J. Looky, R. M. Supkowski, W. D. Horrocks, T. J. Mc Murry, R. B. Lauffer, *J. Am. Chem. Soc.* **2002**, *124*, 3152–3162.
[132] K. Adzamli, L. Vander Elst, S. Laurent, R. N. Muller, *Magn. Reson. Mater. Phys. Biol. Med.* **2001**, *12*, 92–95.
[133] V. Henrotte, *Approche multiple de l'étude quantitative des interactions non covalentes entre macromolécules biologiques et petits ligands*, Ph. D. Thesis, UMH, **2006**.
[134] S. Aime, M. Chiaussa, G. Digilio, E. Gianolio, E. Terreno, *J. Biol. Inorg. Chem.* **1999**, *4*, 766–774.
[135] S. Aime, P. L. Anelli, F. Fedeli, S. G. Crich, M. Murru, E. Terreno, *ISMRM Meeting Abstracts*, Nice, France, **1995**, p. 1096.
[136] T. N. Parac-Vogt, K. Kimpe, S. Laurent, L. Vander Elst, C. Burtea, F. Chen, R. N. Muller, Y. Ni, A. Verbruggen, K. Binnemans, *Chem. Eur. J.* **2005**, *11*, 3077–3086.
[137] J. Kotek, P. Lebduskova, P. Hermann, L. Vander Elst, R. N. Muller, C. F. Geraldes, T. Maschmeyer, I. Lukes, J. A. Peters, *Chem. Eur. J.* **2003**, *9*, 5899–5915.
[138] C. Henoumont, V. Henrotte, S. Laurent, L. Vander Elst, R. N. Muller, *J. Inorg. Biochem.* **2008**, *102*, 721–730.
[139] C. Henoumont, L. Vander Elst, S. Laurent, R. N. Muller, *J. Phys. Chem. B* **2010**, *114*, 3689–3697.
[140] S. Aime, M. Botta, M. Fasano, S. G. Crich, E. Terreno, *J. Biol. Inorg. Chem.* **1996**, *1*, 312–319.
[141] R. Hovland, A. J. Aasen, J. Klaveness, *Org. Biomol. Chem.* **2003**, *1*, 1707–1710.
[142] P. L. Anelli, L. Lattuada, V. Lorusso, M. Schneider, H. Tournier, F. Uggeri, *Magn. Reson. Mater. Phys. Biol. Med.* **2001**, *12*, 114–120.
[143] H. Tournier, B. Lamy, R. Hyacinthe, PCT Int. Appl., WO 9700087, **1997**.
[144] K. Kimpe, T. N. Parac-Vogt, S. Laurent, C. Piérart, L. Vander Elst, R. N. Muller, K. Binnemans, *Eur. J. Inorg. Chem.* **2003**, 3021–3027.
[145] T. N. Parac-Vogt, K. Kimpe, S. Laurent, C. Piérart, L. Vander Elst, R. N. Muller, K. Binnemans, *Eur. J. Inorg. Chem.* **2004**, 3538–3543.
[146] C. Tilcock, E. Unger, P. Cullins, P. MacDougall, *Radiology* **1989**, *171*, 77–80.
[147] G. Kabalka, E. Buonocore, K. Hubner, T. Moss, N. Norley, L. Huang, *Radiology* **1987**, *163*, 255–258.
[148] S. Laurent, L. Vander Elst, C. Thirifays, R. N. Muller, *Eur. Biophys. J.* **2008**, *37*, 1007–1014.
[149] S. Laurent, L. Vander Elst, C. Thirifays, R. N. Muller, *Langmuir* **2008**, *24*, 4347–4351.
[150] T. N. Vogt, K. Kimpe, S. Laurent, C. Pierart, L. Vander Elst, R. N. Muller, K. Binnemans, *Eur. Biophys. J.* **2005**, 1–9.
[151] I. Bertini, F. Bianchi, L. Calorini, S. Colagrande, M. Fragai, A. Franchi, O. Gallo, C. Gavazzi, C. Luchinat, *Magn. Reson. Med.* **2004**, *52*, 669–672.
[152] L. Lattuada, G. Lux, *Tetrahedron Lett.* **2003**, *44*, 3893–3895.
[153] G. J. Strijkers, W. J. Mulder, R. B. van Heeswijk, P. M. Frederik, P. Bomans, P. C. Magusin, K. Nicolay, *Magn. Reson. Mater. Phys., Biol. Med.* **2005**, *18*, 186–192.
[154] K. E. Lokling, R. Skurtveit, A. Bjornerud, S. L. Fossheim, *Magn. Reson. Med.* **2004**, *51*, 688–696.
[155] K. E. Lokling, S. L. Fossheim, J. Klaveness, R. Skurtveit, *J. Contr. Release* **2004**, *98*, 87–95.
[156] L. Frich, A. Bjornerud, S. Fossheim, T. Tillung, I. Gladhaug, *Magn. Reson. Med.* **2004**, *52*, 1302–1309.
[157] L. H. Lindner, H. M. Reinl, M. Schlemmer, R. Stahl, M. Peller, *Int. J. Hyperthermia* **2005**, *21*, 575–588.

Received: November 3, 2011
Published Online: February 27, 2012

